SEISMOLOGICAL RESEARCH IN CENTRAL ALASKA

N. N. Biswas, et al

Alaska University

Prepared for:

Air Force Office of Scientific Research
Advanced Research Projects Agency

December 1974

UNCLASSIFIED

SECURITY CLASSIFICATION OF THIS PAGE (When Data Entered)

REPORT DOCUMENTATION PAGE	READ INSTRUCTIONS BEFORE COMPLETING FORM
1. REPORT NUMBER	2. GOVT ACCESSION NO. 3. RECIPIENT'S CATALOG NUMBER: ADA009 161
4. TITLE (and Subtitle): SEISMOLOGICAL RESEARCH IN CENTRAL ALASKA	5. TYPE OF REPORT & PERIOD COVERED: FINAL 1 APR 1973 - 31 DEC 1974
	6. PERFORMING ORG. REPORT NUMBER
7. AUTHOR(s): N. N. Biswas, B. Bhattacharya, J. D. VanWormer, J. Davies, L. Gedney	8. CONTRACT OR GRANT NUMBER(s): F44620-73-C-0053
9. PERFORMING ORGANIZATION NAME AND ADDRESS: Geophysical Institute, University of Alaska, Fairbanks, Alaska 99701	10. PROGRAM ELEMENT, PROJECT, TASK AREA & WORK UNIT NUMBERS: 62701E AO 1827
11. CONTROLLING OFFICE NAME AND ADDRESS: Advanced Research Projects Agency/NMR 1400 Wilson Boulevard Arlington, VA 22209	12. REPORT DATE: Dec 1974
	13. NUMBER OF PAGES: 87
14. MONITORING AGENCY NAME & ADDRESS (if different from Controlling Office): Air Force Office of Scientific Research/NP 1400 Wilson Boulevard Arlington, VA 22209	15. SECURITY CLASS. (of this report): UNCLASSIFIED
	15a. DECLASSIFICATION DOWNGRADING SCHEDULE

16. DISTRIBUTION STATEMENT (of this Report)

Approved for public release; distribution unlimited.

17. DISTRIBUTION STATEMENT (of the abstract entered in Block 20, if different from Report)

18. SUPPLEMENTARY NOTES

19. KEY WORDS (Continue on reverse side if necessary and identify by block number)

P-WAVE, UPPER MANTLE PHASES, CRUSTAL P-PHASES, PLATE TECTONICS, EARTHQUAKE SOURCE MECHANICS, EARTHQUAKE MAGNITUDE, EXPLOSION MAGNITUDE

20. ABSTRACT (Continue on reverse side if necessary and identify by block number)

The results of studies of four related seismological problems are presented. The data analyzed for these studies were obtained by the central Alaskan seismic networks (Geophysical Institute, NOAA). The first problem deals with the regional P-wave travel-time relations in the epicentral distance range of 100 to 4500 km. The data showed linear fit to five travel-time branches with apparent velocities of 7.05, 8.07, 8.29, 10.39 and 12.58 km/sec, respectively. A tentative average depth of 46 km for the M-discontinuity in central Alaska

DD FORM 1 JAN 73 1473 EDITION OF 1 NOV 65 IS OBSOLETE

UNCLASSIFIED

SECURITY CLASSIFICATION OF THIS PAGE (When Data Entered)

has been suggested. The 400 and 600 km discontinuity in the upper mantle have been correlated with the sharp changes in travel-time gradients at 1900 and 2850 km, respectively.

The second problem deals with the morphology of the Benioff zone in southcentral Alaska. The results show that the underthrust North Pacific lithospheric plate extends north up to about 63°N across the Alaska Range. Also the plate shows a possible break under the Yentna River Prince Willam Sound area.

The third problem deals with the P-wave first-motion solutions of small magnitude earthquakes located in central Alaska. The earthquakes with focal depths less than 60 km show either strike-slip or normal faulting focal mechanism, while those with focal depths greater than the above value show nearly pure dip-slip motions. The solutions, in general, show a northwest-southeast trend of the pressure axes. Also the regional features of the focal mechanism show good correlation with those predicted from North Pacific plate tectonics.

The fourth problem deals with the surface and body wave magnitude relations for earthquakes and explosions for two regions, Nevada-California and central Aleutian. In the M_s-m_b relations, the earthquakes from both the areas show clear separation from the explosions.

TABLE OF CONTENTS

	Page
Acknowledgements	v
Section 1	
Travel Time Relations for the Crust and Upper Mantle P-Wave Phases for Central Alaskan Data, by N. N. Biswas and B. Bhattacharya	
Abstract	1
Introduction	2
Results	6
Conclusions	13
References	16
Table and Figure Captions	18
Section 2	
Seismicity and Plate Tectonics in South-Central Alaska, by J. D. VanWormer, J. Davies and L. Gedney	
Abstract	25
Introduction	26
Data Analysis and Interpretation	29
Conclusions	32
References	35
Figure Captions	38
Section 3	
Earthquake Source Mechanics for Small Magnitude Earthquakes in Central Alaska, by B. Bhattacharya and N. N. Biswas	
Abstract	45
Introduction	46
Data	47
Results	48
Discussion	51
Conclusions	53
References	59

Section 3 (Cont'd) Page

Table Captions 60

Figure Captions 61

Section 4

Study of Ms-m_b Relations from Central Alaska Data, by N. N. Biswas and B. Bhattacharya

Abstract 73

Introduction 74

Data 75

Results 76

Conclusions 78

References 79

Figure Captions 80

ACKNOWLEDGEMENTS

Part of this research was supported by the Advanced Research Projects Agency of the Department of Defence and was monitored by the Air Force Office of Scientific Research under Contract No. F44620-73-C-0053.

We gratefully acknowledge the continued interest and support of Mr. W. G. Best of the Air Force Office of Scientific Research. We express our appreciation to the following personnel for their cooperation:

Mr. Jack Townsend, College Observatory, USGS, College, Alaska,
Mr. Robert Eppley, National Weather Service, Palmer Observatory, Palmer, Alaska,
Mr. Glenn Roberts, Summit Weather Service, Alaska

1. TRAVEL-TIME RELATIONS FOR THE CRUST AND UPPER MANTLE P-WAVE PHASES FROM CENTRAL ALASKAN DATA

By N. N. Biswas and B. Bhattacharya

ABSTRACT

This section of the report deals with the travel-time relations for the crust and upper mantle P-wave phases in the epicentral distance range of 100 to 4500 km. The short-period data analyzed were from underground nuclear explosions in the central Aleutian and Nevada regions, from earthquakes located in central and southcentral Alaska and along the north Pacific seismic belts; the data were recorded by the interior Alaskan seismic network.

In the epicentral distance range of 100 to 600 km, the first arrival P-wave phases are P* and P_n; the former has been identified as the earliest arrival for $\Delta<300$ km with an apparent velocity of 7.05 km/sec while for epicentral distances greater than 300 km, the latter phase arrives first and shows an apparent velocity of 8.07 km/sec. A tentative Mohc depth of 46 km for central Alaska has been obtained from this study. This value is in close agreement with that derived for southern Alaska by others.

The data for the epicentral distance range of 700 to 4500 km could be explained by three linear relations: the first extends from 700 to 1900 km with apparent velocity of 8.29 km/sec, the second lies between 1900 and 2850 km with apparent velocity of 10.39 km/sec, and the third extends from 2850 to 4500 km with apparent velocity of 12.58 km/sec.

In the epicentral distance range of 1900 to 2600 km, the first P-wave arrivals from earthquakes in the Aleutian area were found to be systematically late by 3 to 4 sec compared with those from central Aleutian underground

nuclear explosions. This discrepancy in travel times has been interpreted as due to mislocations and errors in origin time for earthquakes in the above area. Also, the well known 400 and 600 km discontinuities in the upper mantle have been correlated with the sharp changes in travel-time gradients at 1900 and 2850 km, respectively.

INTRODUCTION

The object of this study was to derive the regionalized travel-time relations for the crust and upper mantle P-wave phases from the data gathered by the local seismological network. Because of the unavoidable source-receiver disposition, most of the travel paths considered for the upper mantle phases, except for P_n, traverse the complex northern portion of the Circum-Pacific seismic belt. For the basal crustal phase P* and upper mantle phase P_n, the earthquakes selected lie within the perimeter of the local seismological network. Due to large scatter in travel-time data for short epicentral distances (Δ<100 km) we could not study the intermediate crustal phase P_g. We anticipate resolving the characteristics of this phase from chemical explosions planned to be carried out by the United States Geological Survey sometime next year.

The events considered for this study which lie along the Alaskan coastal belt on the south and southwest of the seismic network are located along the well known deep sea trench-island arc system. The predominant feature of this system is a lithospheric plate sinking into the upper mantle, which is characterized by a low-velocity zone, phase change, and rapid velocity variation. The seismicity indicates a variable dip of the sinking lithosphere, namely 40° to 50° in southern Alaska-central Aleutian region, 50° to 60° on the west of Rat Island and 90° at

the western end of the Aleutian arc (Jacob, 1972; Davies and Julian, 1972; Engdahl, 1973). Farther west along the Kurile-Kamchatka seismic zone, the underthrust plate strikes in the northeast-southwest direction with a dip of the order of 50° to 60° due northwest (Fedotov, 1968). The above regional geometry of the plate is in accord with that derived from the relative motion of the North Pacific plate with respect to the American plate along the southern Alaska-Aleutian region and the former and the Eurasian plate along the Kurile-Kamchatka region (McKenzie and Parker, 1967; Le Pichon, 1968; Stauder, 1968a, b, 1972).

Epicenters of earthquakes with focal depths between 100 and 200 km located along the trench-arc system show positive correlation with the positions of active andesite volcanoes. Le Pichon et al. (1973) summarized important results concerning the interrelationships of various features observed along the plate boundaries. Moreover, several authors (Sorrells et al., 1971; Toksöz et al., 1971; Jacob, 1972; Davies and Julian, 1972; Abe, 1972; Sleep, 1973) derived models for the sinking lithosphere. For the central Aleutian arcs, Jacob (1972) proposed a model in which the sinking plate reaches a depth of 250 km from the surface with 7 to 10 per cent higher P-wave velocity than the surrounding medium; the thickness of the plate was shown to be 80 km. Quite similar models have been considered by Davies and Julian (1972) and Sleep (1973) for their studies of the explosion data from Amchitka Island. The close similarity of seismicity between the central Aleutian and Kurile-Kamchatka seismic zones perhaps indicates the structure of the dipping plate under the latter area as similar to that proposed for the former area by Jacob and others.

The source region on the southeast of the seismic networks belong to the well known strike-slip fault systems marking the contact planes between the Pacific and American plates. Besides the Nevada underground nuclear explosions, these events were chosen to compare the P-wave travel times observed in central Alaska for propagation paths outside the deep sea trench-island arc system. The results have been discussed in later sections.

The receiver region is also complex; the major structural trends south of 64°N as shown in Figure 1, are predominantly strike-slip faults which parallel the broad arcuate structure of the Alaska Range. Previous geophysical studies (Woollard et al., 1960; Hanson et al., 1968) indicate the presence of a mountain root under the above range. The summary of Alaskan seismicity (Tarr, 1970) shows the extension of the Aleutian seismic belt in interior Alaska where it widens and spreads over a region of about 750 km across. The hypocenters of earthquakes decrease in depth from about 150 km in the Cook Inlet area to less than 50 km along the northern and eastern margins of the inland active seismic zone.

Davies and Berg (1973) have provided evidence of a sharp westward dip of the M-discontinuity just north of Cook Inlet. From hypocenter distribution of earthquakes in central Alaska, Van Wormer et al. (1974) showed the termination of the Benioff zone in interior Alaska some 75 km north of the Denali fault. They also found the possibility of a break in the subducting lithospheric plate in the Yenta River-Prince William Sound area. Lahr et al. (1974) and Lahr (1974) made similar studies with improved seismic control around Cook Inlet. They obtained a westward

dipping Benioff zone reaching a depth of 150 km from the surface in the above area. The seismic zone along the sinking lithosphere in the depth range of 50 to 150 km was shown to have a thickness of about 15 to 20 km. It seems that further reduction in location errors may show the true thickness of the seismic zone smaller than these values (Engdahl, 1973).

Carder et al. (1967) reported the seismic body-wave arrivals in the distance range of 0° to 27° from the nuclear explosion LONGSHOT on Amchitka Island. During two latexplosions (MILROW and CANNIKIN), a number of permanent and semi-permanent seismic short-period stations were operated by a number of federal and state agencies. Biswas (1973) reported the distribution of the observed P-wave travel-time residuals in the Alaska-Aleutian region by combining data from all three nuclear explosions. The results are shown in Figure 2; the values in parentheses are mean residuals ($\delta t = \langle t_o - t_h \rangle$), where t_o is the depth-ellipticity corrected observed travel time and t_h is the corresponding value of Herrin et al. (1968) for a given epicentral distance.

The time residuals indicate that for propagation from the central Aleutian area, the P arrivals are systematically early in central Alaska to the east of approximately 151°W. These may result from structural complexities either at the source region or at the receiver region or a combination of both. Thus, prior to any further analysis, it is necessary to separate the observed residuals into major components. Studies to determine station residuals from teleseismic events located in different azimuths with respect to central Alaska are in progress. In the following sections, we have discussed the first arrival P-wave travel-time relations in the epicentral distance range of 100 to 4500 km from short-period data obtained by the central Alaskan seismic network.

RESULTS

A. P_n and Crustal P-wave in Central Alaska

Because of the lack of explosion data in large parts of central Alaska for the epicentral distance range in which the crustal phases and P_n are observed as first arrivals, we have based our study to date solely on impulsive first arrivals, we have based our study to date solely on impulsive first arrival P-wave phases from earthquakes (1967 through 1972) distributed inland and on coastal sections of central Alaska. The locations of the epicenters are shown in Figure 3a; the results have been summarized in Figure 3b and 3c.

The location and the origin time of the earthquakes considered for this study, as well as for other studies discussed in later sections were taken from NOAA's Monthly Bulletins (PDE). The observed travel times have been reduced to sea level by applying time corrections for focal depth and receiver elevation. The corrections were obtained either directly from the Herrin table (1968) when focal depths coincided with the table values, or values were interpolated from the above table for appropriate focal depths. Finally, the ellipticity corrections were applied to the depth-corrected travel times from Bullen's tables (1937).

The travel-time data show a break in the gradient around Δ = 300 km. This can be seen clearly in the reduced time plot (Figure 3c). We thus fitted the data by two linear relations in the least-squares sense. For Δ<300km, the linear relation yielded an apparent velocity of 7.05 km/sec and an intercept time of 3.37 sec. The apparent velocity obtained for the P_n phase (Δ<300 km) is 8.07 km/sec and an intercept time of 8.62 sec. The first P-phase appears to represent P*; we have yet to establish the values for P_g for this area as mentioned in the previous section.

Hales and Asada (1966) studied P-wave travel-time relations in the epicentral distance range of 80 to 400 km in southern Alaska. The sources were a series of chemical explosions located in the Prince William Sound area. Their travel-time relations for the lower crust show an apparent velocity of 6.98 km/sec and an intercept time of 4.2 sec. These agree, within the experimental accuracy, with our results obtained for Δ<300 km. Also, from the analysis of data obtained along a profile close to the Alaska-Canada border, Hales and Asada (1966) obtained an apparent velocity of 8.07 km/sec and an intercept time of 9.1 sec for the P_n phase. Our results for 300 km < Δ < 600 km, though obtained for central and southcentral Alaska, are very similar.

B. Travel Time Relations for the Upper Mantle P-Wave Phases

For this study, short period data collected from 1970 through 1972 by the central Alaskan stations have been analyzed. Records from 146 out of about 340 earthquakes were found with clear impulsive first arrivals and the arrival times could be read within $\pm$ 0.2 sec. The location of the selected events are shown in Figure 4, and regionwise, the ranges of magnitude and focal depth are given in Table 1.

Earthquakes with magnitudes less than the lower bound of Table 1, and originating on the western side of Alaska Peninsula and further west along the island arc structure, show a few cycles of small amplitude precursors as the first arrivals followed by a large amplitude envelope. This phenomenon has been reported before by Jacob (1972) for the LONGSHOT event recorded at Point Barrow. Similar features were observed in western Canadian records from the above event by Davies and Julian (1972) and in LASA records by Davies and Frazer (1970) from Aleutian earthquakes.

Jacob (1972), by employing ray-tracing, suggested that the large amplitude envelope could be either a P-phase refracted from the top of the dipping lithospheric plate along the Aleutian seismic zone, or the P-phase refracted from the 600-km discontinuity. He related the highly attenuated first arrivals to the normal P-phase that propagates just above the plate. Davies and Julian (1972) made similar suggestions for the signal characteristics observed in western Canada, again based on a ray-tracing method for the LONGSHOT event.

We have examined records for a large number of Aleutian earthquakes obtained by central Alaskan stations having high- and low-gain recording channels. Frequently, the high-gain trace shows a distinct impulsive first break, thereby minimizing the reading error to $\pm$ 0.2 sec while the low-gain trace shows a precursor to the main signal. Our results discussed below are based solely on impulsive first arrivals.

The depth-ellipticity corrected travel times are shown in Figure 5 as a function of the epicentral distance in the range of 700 to 4500 km; the plot of the reduced travel time is shown in Figure 6. In these figures, we have also included travel-time data for impulsive first P-arrivals from three nuclear tests on Amchitka Island, from five nuclear tests in Nevada and from a few selected earthquakes located in the southeastern azimuth with respect to the central Alaskan seismic network. It should be noted that the locations and origin times of earthquakes were obtained using the Jeffreys-Bullen tables, whereas those values are known for the explosions. Thus the travel times for earthquakes are subject to additional uncertainties because of errors in locations and origin times. The travel-time values corresponding to the explosions

and southeastern events are shown in Figures 5 and 6 by crosses and hollow triangles, respectively. We incorporated data from southeastern events for reasons mentioned in previous sections.

A number of interesting features, as discussed below, can be observed particularly in the reduced travel-time plot (Figure 6).

As the epicentral distance increases, the scatter in the data decreases. This feature becomes apparent for $\Delta > 2500$ km and may be explained by the fact that the errors contributed by location uncertainties or the fluctuations in travel-time values caused by structural heterogeneities or a combination of both, become small compared to the true travel times for large epicentral distances.

In the epicentral distance range of $2100 < \Delta < 2500$ km, the travel times for earthquakes are systematically late by 3 to 4 sec compared to those from explosions. The locations of the events with respect to the central Alaskan seismic network of stations for the above distance range extend from about 162°W to the western end of the Aleutian seismic zone. It is well known that the location of LONGSHOT, using the usual location methods with teleseismic data, revealed considerable errors in computed values of the focal depth, position of the epicenter and origin time. The details can be found in Tables 1 and 2 of Lambert et al. (Vol. 2, 1970). When the focal depth was constrained to zero, the authors found a northward shift by 20 km in the computed position of the epicenter from the true site. Engdahl (1973) relocated a number of intermediate depth earthquakes in the central Aleutian area from data obtained by a local seismic network. He found the hypocenters were displaced by 30 km upward compared with those determined from the usual location method. An error in epicenter location by $\pm$ 20 km, or in focal depth by $\pm$ 30 km,

introduces an uncertainty of $\pm$ 2 to $\pm$ 3 sec in travel time at $\Delta \sim 2200$ km, the epicentral distance common for the Aleutian events from central Alaskan stations.

In view of the above results, it is suggested that the observed discrepancy in travel times between earthquakes and explosions in the epicentral distance range of 1900 to 2600 km is mainly due to systematic errors in the reported values (PDE: location and origin time) for the Aleutian earthquakes. This interpretation seems necessary but may not be sufficient, as refraction of the rays emerging in central Alaska by the sub-Aleutian lithospheric slab may partially or totally invalidate the great-circle travel path assumption, a factor inherent in our analysis.

In the epicentral distance range of 700 to 1900 km, 19 reliable data points from underground nuclear explosions on Amchitka Island were available. These data have been supplemented by high-quality data from earthquakes located in the southeast, south and southwest directions with respect to central Alaska. The results show (Figures 5 and 6) that, at least to the present accuracy of our measurements, the first-arrival travel times for the above epicentral distance range cannot be grouped on the basis of the direction of propagation alone, as the data, in addition to following a single linear trend, exhibit comparable scatter from all three azimuths. However, the range of scatter may be reduced by incorporating station corrections currently not available for the stations used in this study.

In the epicenter distance range of about 3400 to 4000 km, the travel-time values for explosions are from underground nuclear tests in Nevada. These are in agreement with those from earthquakes approximately

in the same azimuth. The rest of the values between 2600 and 4500 km were obtained from earthquakes located in western Aleutian and Kurile-Kamchatka seismic zones. These values are also in close agreement with those from the southeastern azimuth, although the travel paths traverse dissimilar tectonic settings.

The travel-time plot as shown in Figure 5 shows three linear segments marked by two sharp changes in gradient, one around 2000 km and the other around 2600 km. These can be seen clearly in the reduced time plot (Figure 6). We have therefore obtained three best-fit linear relations by the least-squares method to explain the data from 700 to 4500 km. In the distance ranges of 700 to 1900 km and 2600 to 4500 km, we have used all available data for the best-fit relations, while between 2050 and 2550 km we have used the earthquake and explosion values separately. The best-fit relations are given below

$$t = (11.71 \pm 0.040) + \Delta/(8.29 \pm 0.002), \quad 700 < \Delta < 1900 \qquad (1)$$

Earthquake Data

$$t = (63.37 \pm 0.250) + \Delta/(10.44 \pm 0.011), \qquad (2a)$$

$$2050 < \Delta < 2550$$

Explosion Data

$$t = (58.43 \pm 0.711) + \Delta/(10.39 \pm 0.033), \qquad (2b)$$

$$t = (106.96 \pm 0.062) + \Delta/(12.58 \pm 0.002), \quad 2600 < \Delta < 4500 \qquad (3)$$

where Δ is in kilometers. The plots of the above relations are shown by solid lines in Figures 5 and 6. The difference in apparent velocities in equations (2a) and (2b) is negligible. This is expected from the parallelism of the two sets of values; however, for reasons discussed previously, the relation in equation (2b) should be preferred in the epicentral distance range in question.

Hales (1972) summarized the results of the seismic refraction studies in the United States and Canada from the Early Rise and NTS

explosion sources. He suggested that between 600 and 700 km, the first arrival P_n branch breaks off to a new travel-time branch with an apparent velocity in the range of 8.35 to 8.45 km/sec. This branch extends up to 2100 km and yields an intercept time from 10 to 13 sec. The next travel-time branch extends from 2100 to 2500 km with an apparent velocity of approximately 10.0 km/sec and an intercept time of about 58 sec. The third branch (Green and Hales, 1968) beyond 2500 km shows an apparent velocity of 12.2 km/sec and an intercept time of 98.5 sec. The breaks at epicentral distances 2100 and 2500 km have been related to the 400 and 600 km discontinuities, respectively. These results indicate the order of magnitude of the apparent P-wave velocities and intercept times which could be expected on a regional basis in the epicentral distance ranges in question.

The results presented from this study permit a qualitative comparison with those cited above and it can be seen that the quantities in equations (1), (2b) and (3), which are representative mean values over the travel paths involved, show close agreement with the regional values. Also, it is important to note that in absence of the explosion data in the epicentral distance range of about 2000 and 2600 km, one would be inclined to relate the sharp changes in gradients at 2100 and 2600 km with the 400 and 600 km discontinuities, respectively. On the other hand, because of errors in location and origin time for earthquakes and considerable uncertainties in travel times resulting from these sources for Aleutian earthquakes, we would correlate the 400 km discontinuity with the change in travel-time gradient at 1900 km and the 600 km discontinuity with the one at 2850 km.

CONCLUSIONS

We cannot yet characterize all the crustal P-wave phases from local earthquakes in central Alaska, due to high scatter in data. We hope to resolve this problem with planned future explosions in the area of interest. However, the results obtained for the basal crustal phase P* and P_n could be considered as a representative mean for the central and southcentral Alaska.

The travel-time relations for the upper mantle P-wave phases obtained from this study are based on source-receiver configurations which involved travel paths through different structural provinces. Besides this unavoidable factor, mislocations and errors in origin time of earthquakes are probably main sources of scatter in data. However, the inclusion of data from underground nuclear explosions for all three travel-time branches provided a reasonable basis to obtain the apparent velocities of 8.29, 10.39 and 12.58 km/sec for the epicentral distance ranges of 700 to 1900 km, 1900 to 2850 km and 2850 to 4500 km, respectively. They are consistent with regional values as cited in the literature. We make no statement about the presence or absence of the P-LVZ in the upper mantle at this stage of our studies.

The travel times for the Aleutian earthquakes as recorded in central Alaska are systematically late by 3 to 4 sec compared with those for underground nuclear explosions on Amchitka Island. By considering krown results, we have interpreted this feature as being due primarily to mislocations and errors in origin time of earthquakes in that area; the earthquakes were systematically located either deeper than true focal depths or farther west from true epicenters or a combination of both.

The well known 400 and 600 km upper mantle discontinuities have been usually identified with the breaks in travel-time gradients at epicentral distances of 2100 and 2600 km, respectively. In the absence of available explosion data, one would draw similar conclusions as above from our results. However, weighing exclusively in favor of explosion data, we correlated the above discontinuities with the breaks in travel-time gradients at 1900 and 2850 km. Nevertheless, their exact positions must be confirmed by incorporating amplitude data besides travel times and inverting the observed results in terms of a realistic earth model. These studies are in progress and the results will be reported in the future.

TABLE I

REGION	NO. OF EVENTS	FOCAL DEPTH (KM)	MAGNITUDE
California	3	$9 \leq h \leq 14$	$5.1 \leq m_b \leq 6.2$
Off-Coast of British Columbia	8	$12 \leq h \leq 33$	$4.6 \leq m_b \leq 5.9$
Southeastern Alaska	3	$18 \leq h \leq 25$	$5.1 \leq m_b \leq 6.5$
Gulf of Alaska and Southern Alaska	12	$21 \leq h \leq 126$	$4.0 \leq m_b \leq 5.8$
			majority $m_b > 4.5$
Alaska Peninsula	3	$20 \leq h \leq 28$	$4.8 \leq m_b \leq 5.2$
Aleutian Islands	5	$11 \leq h \leq 29$	$5.0 \leq m_b \leq 6.0$
	39	$32 \leq h \leq 60$	$4.6 \leq m_b \leq 6.0$
			majority $m_b > 5.0$
	10	$62 \leq h \leq 107$	$5.1 \leq m_b \leq 6.0$
Kurile Islands and Kamchatka	5	$15 \leq h \leq 30$	$5.1 \leq m_b \leq 6.2$
	22	$32 \leq h \leq 60$	$5.0 \leq m_b \leq 6.1$
	3	$81 \leq h \leq 134$	$5.0 \leq m_b \leq 6.3$

REFERENCES

Biswas, N. N. (1973). P-wave travel-time anomalies: Aleutian-Alaska region, Tectonophysics, 19, 361-367.

Biswas, N. N. and B. Bhattacharya (1974). Travel-time relations for the upper mantle P-wave phases from central Alaskan data, Bull. Seism. Soc. Am., 64 (in press).

Carder, D. S., D. Tocher, C. Bufe, S. W. Steward, J. Eisler and E. Berg (1967). Seismic wave arrivals from LONGSHOT, 0° to 27°, Bull. Seism. Soc. Am., 57, 573-590.

Davies, D. and C. W. Frasier (1970). P-wave multipathing, seismic discrimination, Semi-Annual Technical Summary, Lincoln Laboratory.

Davies, D. and B. R. Julian (1972). A study of short-period p-wave signals from Longshot, Geophys. J., 29, 185-202.

Davies, J. and E. Berg (1973). Crustal morphology and plate tectonics in southcentral Alaska, Bull. Seism. Soc. Am., 63, 673-677.

Engdahl, E. R. (1973). Relocation of intermediate depth earthquakes in central Aleutians by seismic ray tracing, Nature, 245, 23-25.

Fedotov, S. A. (1968). On deep structure, properties of the upper mantle, and volcanism of the Kurile-Kamchatka Island are according to seismic data, The Crust and Upper Mantle of the Pacific Area, L. Knopoff, C. L. Drake and P. J. Hart, Editors, Am. Geophys. Union, Washington, D. C.

Green, R. W. E. and A. L. Hales (1968). The travel times of P waves to 30° in the central United States and upper mantle structure, Bull. Seism. Soc. Am., 58, 267-289.

Hales, A. L. and T. Asada (1966). Crustal structure in coastal Alaska, in The Earth Beneath the Continents, AGU Geophysical Monograph, 10, 420-432.

Hales, A. L. (1972). The travel times of P seismic waves and their relevance to the upper mantle velocity distribution, in the Upper Mantle, A. R. Ritsema, Editor, Elsevier Publishing Co.

Hanson, K., E. Berg and L. Gedney (1968). A seismic refraction profile and crustal structure in central interior Alaska, Bull. Seism. Soc. Am., 58, 1657-1665.

Herrin, E., E. P. Arnold, B. A. Bolt, G. E. Clawson, E. R. Engdahl, H. W. Freedman, D. W. Gordon, A. L. Hales, J. L. Lobdell, O. Nuttli, C. Romney, J. Taggart and W. Tucker (1968). Seismological tables for p phases, Bull. Seism. Soc. Am., 58, 1196-1221.

Jacob, K. H. (1972). Global tectonic implications of P travel-times from the nuclear explosion, Longshot, J. Geophys. Res., 77, 2556-2573.

Lahr, J. C., R. A. Page and T. A. Thomas (1974). Catalog of earthquakes in southcentral Alaska, U. S. Geological Survey Open File Report.

Lahr, J. C. (1974). Detailed seismic investigation of Pacific-North American plate interaction in southern Alaska, Ph.D. thesis, Columbia University.

Lambert, D. G., D. H. VonSeggern, S. S. Alexander and S. A. Galat (1970). The Longshot experiment (Vol. 2), Seismic data laboratory report No. 234, Alexandria, Virginia.

Le Pichon, X. (1968). Sea-floor spreading and continental drift, J. Geophys. Res., 73, 3661-3697.

Le Pichon, X., J. Francheteau and J. Bonnin (1973). Plate Tectonics, Elsevier Sci. Pub. Co., New York.

McKenzie, D. P. and R. L. Parker (1967). The North Pacific: an example of tectonics on a sphere, Nature, 216, 1276-1280.

Sleep, N. H. (1973). Teleseismic P-wave transmission through slabs, Bull. Seism. Soc. Am., 63, 1349-1373.

Sorrells, G. G., J. B. Crowley and K. F. Veith (1971). Methods for computing ray path in complex geological structures, Bull. Seism. Soc. Am., 61. 27-52.

Stauder, W. (1968a). Mechanism of the Rat Island earthquake sequence of February 4, 1965 with relation to island arcs and sea-floor spreading, J. Geophys. Res., 73, 3847-3858.

Stauder, W. (1968b). Tensional character of earthquake foci beneath the Aleutian Trench with relation to sea-floor spreading, J. Geophys. Res., 73, 7693-7701.

Stauder, W., Fault motion and spatially bounded character of earthquakes in Amchitka Pass and Delarof Island, J. Geophys. Res., 77, 2072-2080.

Tarr, A. C. (1970). New maps of polar seismicity, Bull. Seism. Soc. Am., 60, 1745-1747.

Toksöz, M. N., J. W. Minear and B. R. Julian (1971). Temperature field and geophysical effects of a downgoing slab, J. Geophys. Res., 76, 1113-1138.

Van Wormer, D., J. Davies and L. Gedney (1974). Seismicity and plate tectonics in southcentral Alaska, Bull. Seism. Soc. Am., 64, 1467-1475.

Woollard, G. P., N. A. Ostenso, E. Thiel and W. E. Bonini (1960). Gravity anomalies, crustal structure and geology in Alaska, J. Geophys. Res., 65, 1021-1037.

TABLE CAPTIONS

Table 1. Ranges of magnitude and focal depth of earthquakes, by region, used in this study.

FIGURE CAPTIONS

Figure 1. Major tectonic features of central Alaska.

Figure 2. P-wave travel time residuals for explosions. The short broken lines indicate the depth and trend of the Aleutian deep seismic zone (Jacob, 1972).

Figure 3. a) Location of epicenters of earthquakes used for P*, P_n study.

b) P-wave travel times for earthquakes for 80 km < Δ < 600 km. The locations and origin times of earthquakes were obtained using the Jeffreys-Bullen tables.

c) Reduced P-wave travel times from earthquakes for 80 km < Δ < 600 km. The locations and origin times of earthquakes were obtained using the Jeffreys-Bullen tables.

Figure 4. Location of epicenters of earthquakes and underground nuclear explosions and short period seismic stations used in this study.

Figure 5. P-wave travel times from earthquakes and explosions for 700 km $\leq\Delta\leq$ 4500 km. The locations and origin times of earthquakes were obtained using the Jeffreys-Bullen tables.

Figure 6. Reduced P-wave travel times from earthquakes and explosions for 700 km $\leq\Delta\leq$ 4500 km. The locations and origin times of earthquakes were obtained using the Jeffreys-Bullen tables.

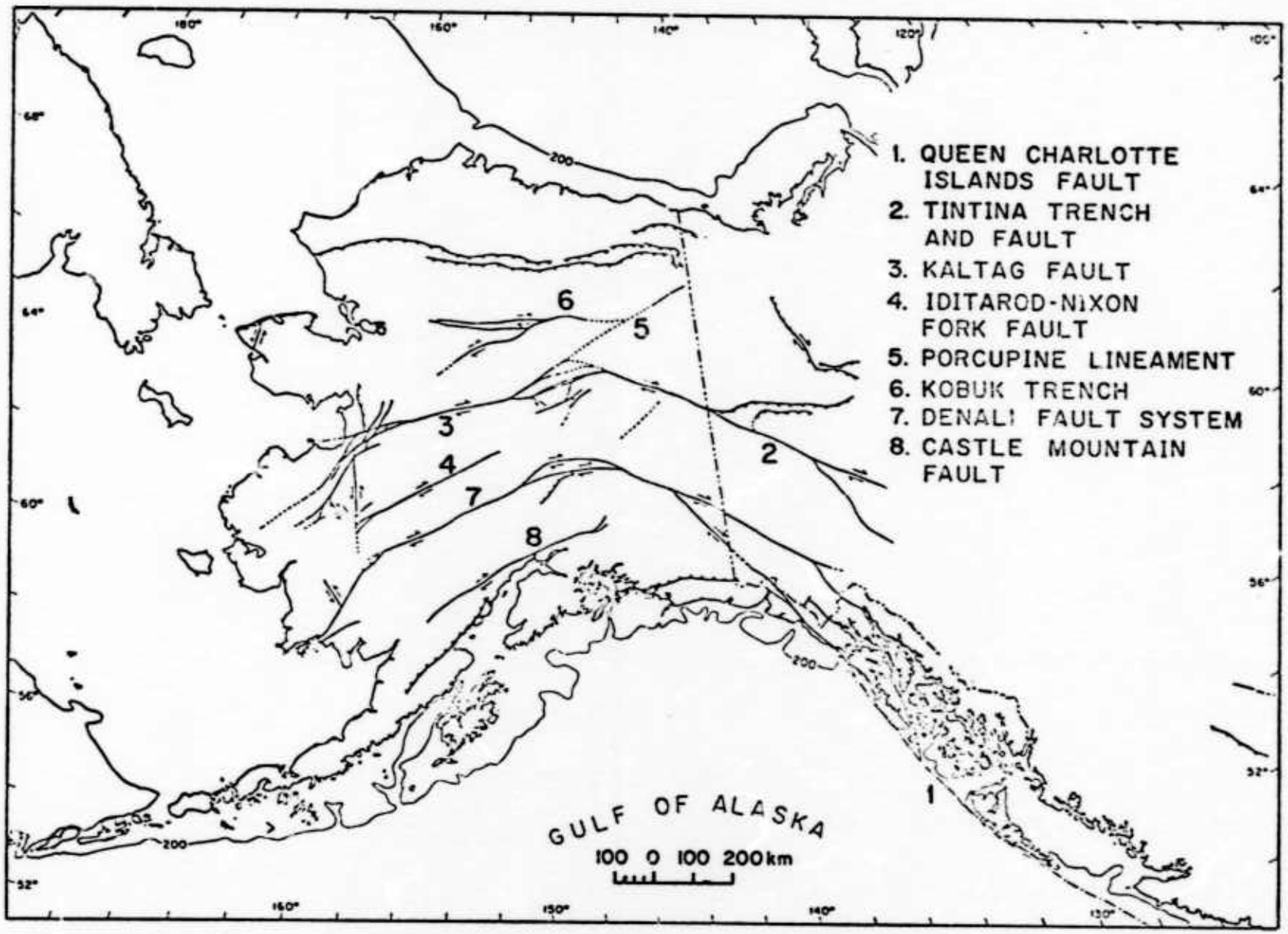

Figure 1. Major tectonic features of central Alaska.

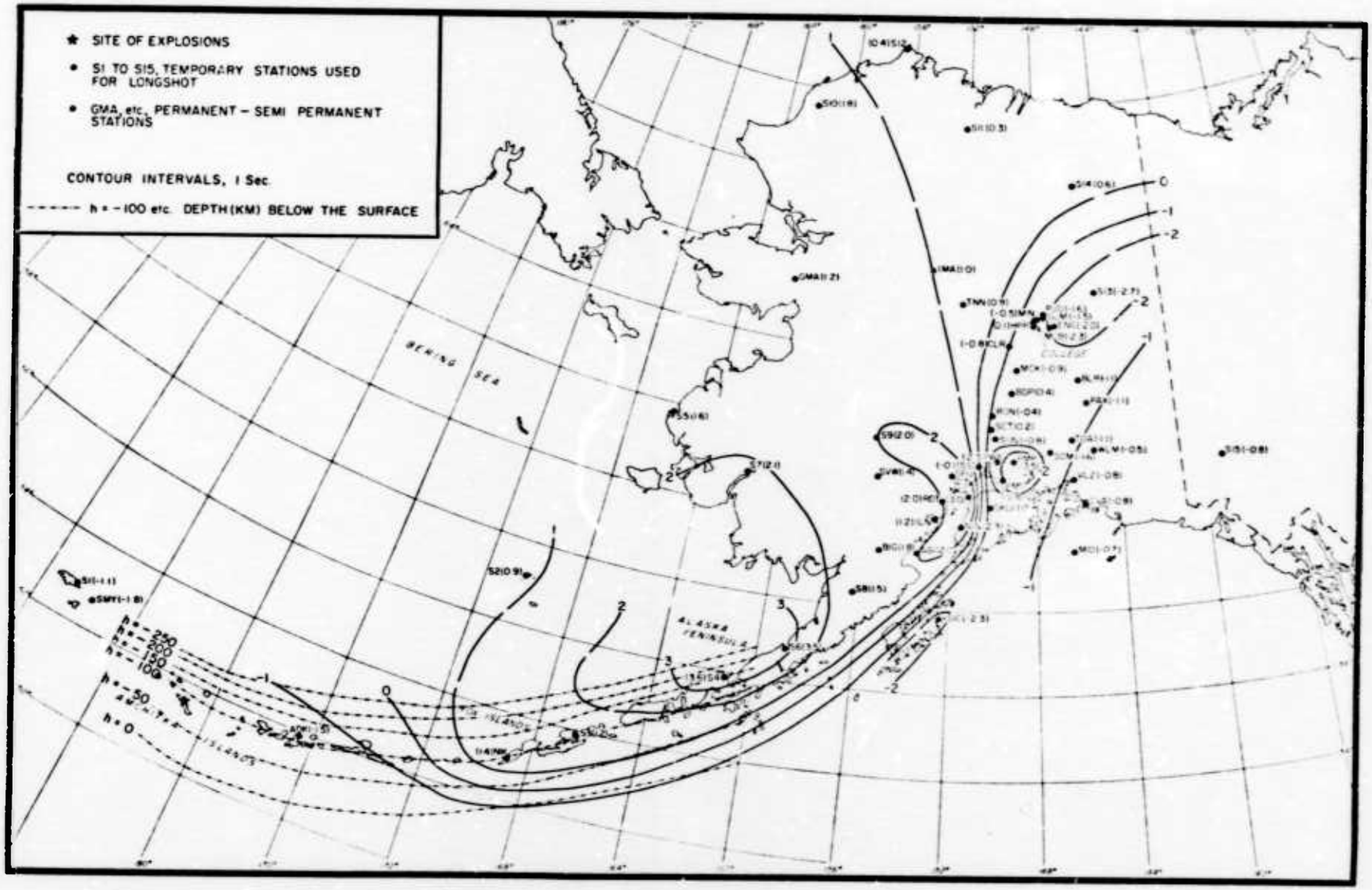

Figure 2. P-wave travel time residuals for explosions. The short broken lines indicate the depth and trend of the Aleutian deep seismic zone (Jacob, 1972).

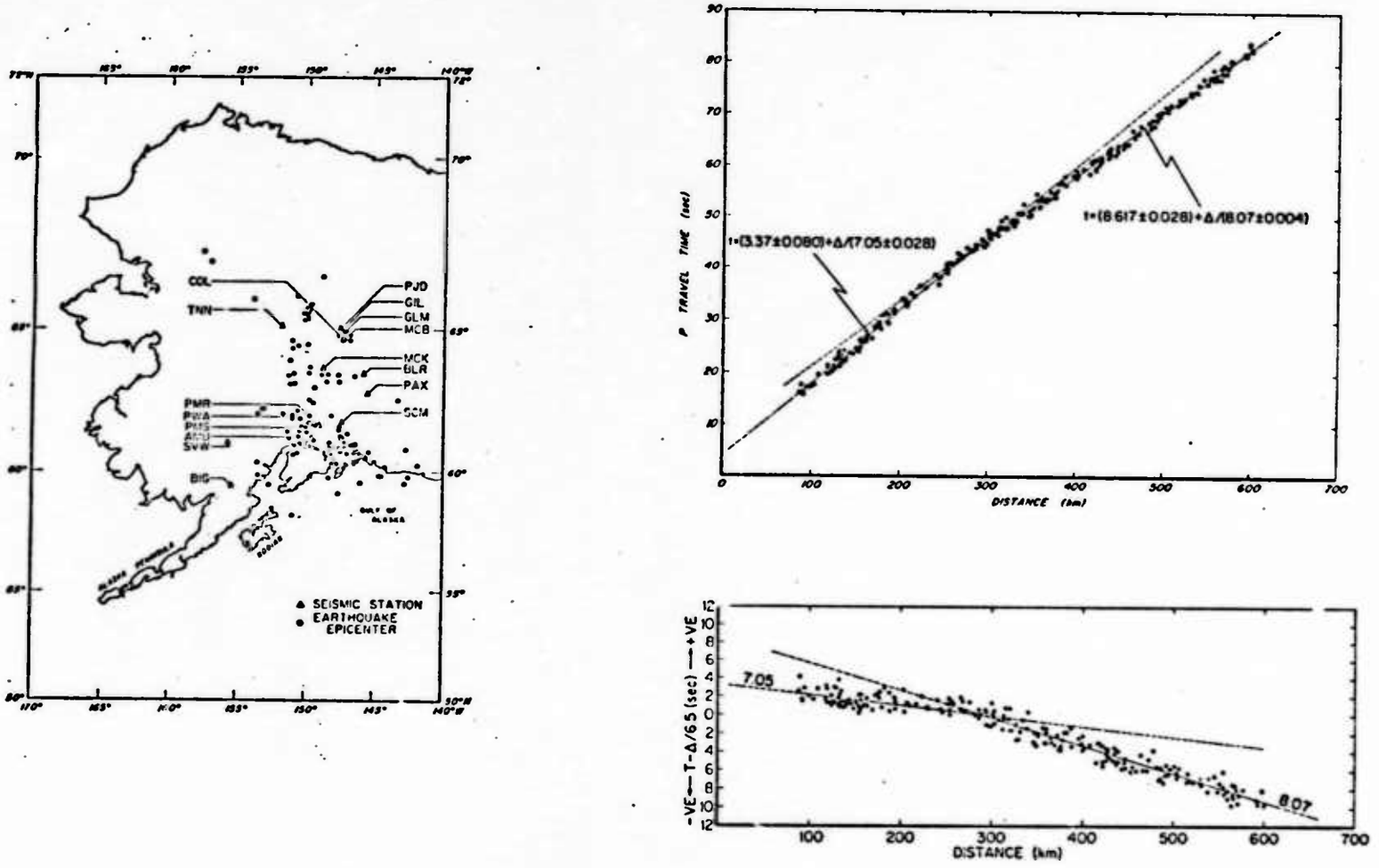

Figure 3. a) Location of epicenters of earthquakes used for P*, P_n study.
b) P-wave travel times for earthquakes for 80 km < Δ < 600 km. The locations and origin times of earthquakes were obtained using the Jeffreys-Bullen tables.
c) Reduced P-wave travel times from earthquakes for 80 km < Δ < 600 km. The locations and origin times of earthquakes were obtained using the Jeffreys-Bullen tables.

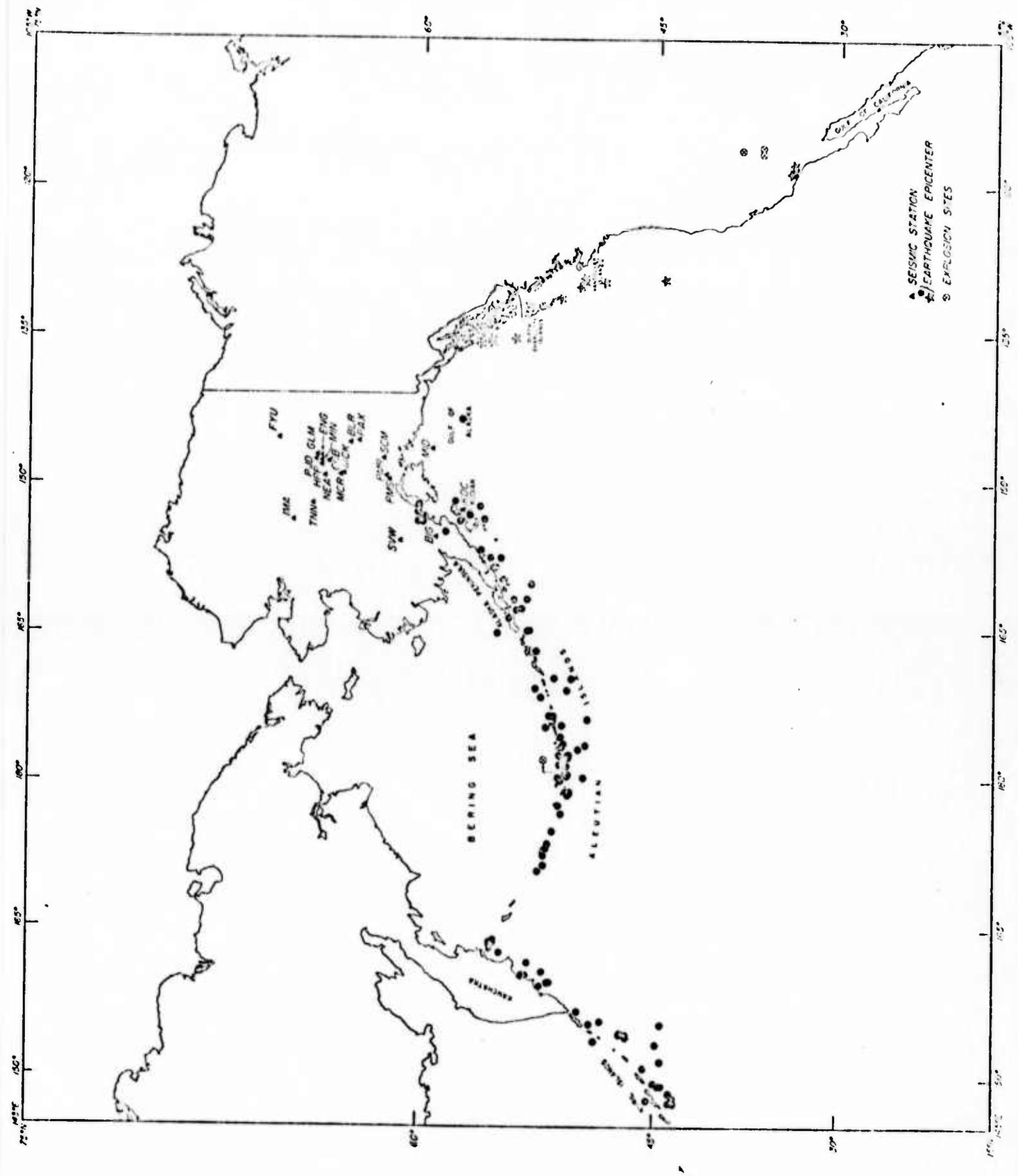

Figure 4. Location of epicenters of earthquakes and underground nuclear explosions and short period seismic stations used in this study.

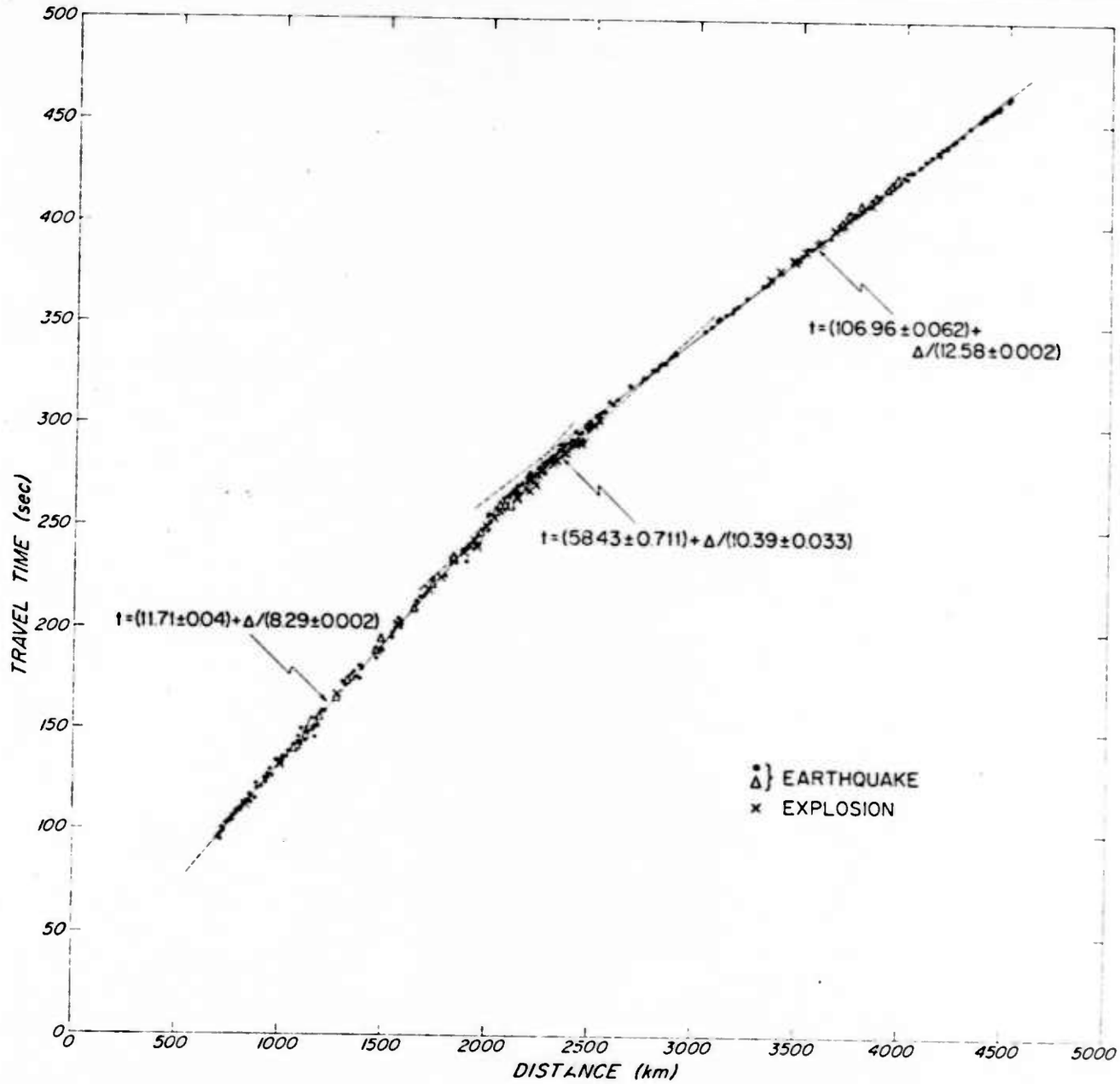

Figure 5. P-wave travel times from earthquakes and explosions for 700 km $\leq\Delta\leq$ 4500 km. The locations and origin times of earthquakes were obtained using the Jeffreys-Bullen tables.

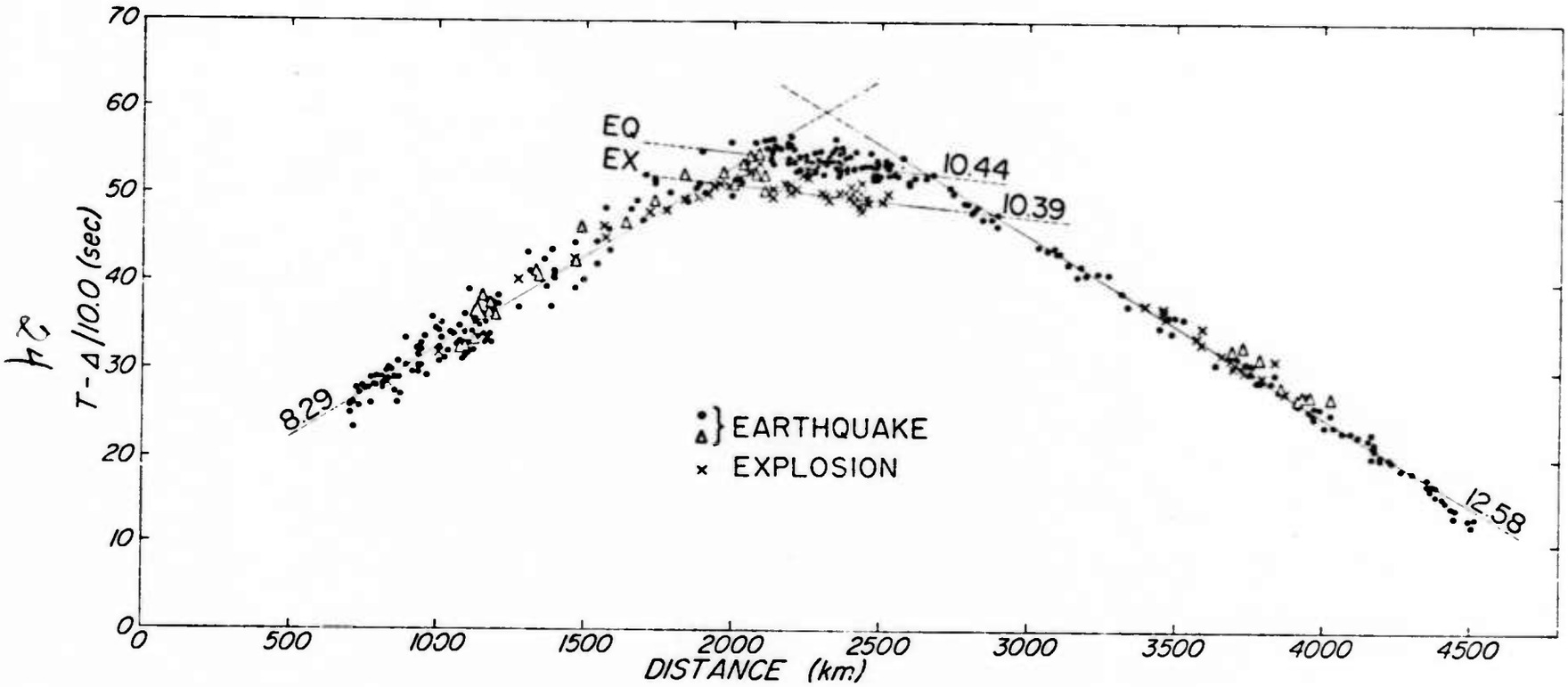

Figure 6. Reduced P-wave travel times from earthquakes and explosions for 700 km $\leq \Delta \leq$ 4500 km. The locations and origin times of earthquakes were obtained using the Jeffreys-Bullen tables.

2. SEISMICITY AND PLATE TECTONICS IN SOUTH CENTRAL ALASKA

By J. D. VanWormer, J. N. Davies and L. D. Gedney

ABSTRACT

Hypocenter distribution shows that the Benioff zone associated with the Aleutian arc terminates in interior Alaska some 75 km north of the Denali fault. There appears to be a break in the subducting Pacific plate in the Yentna River-Prince William Sound area which separates two seismically independent blocks, similar to the segmented structure reported for the central Aleutian arc.

INTRODUCTION

The role of the Aleutian arc and the Denali fault in the tectonics of the northeast Pacific Basin has long been a subject of study and speculation. It is our purpose in this report to discuss the termination of the arc system in the continental block and to present some new data concerning the geometry of the Benioff zone. First we present a brief review of past work, which is intended only to provide background information and is not meant to be a complete bibliography.

The observations and hypotheses of some early workers embodied many of the elements of plate tectonic theory, although it was many years before the concept evolved into the presently popular working hypothesis involving rigid plates. Some twenty years ago Gutenberg and Richter (1954, page 32) commented that "The shallow shocks in the interior of Alaska represent an interior structure, related to the Pacific coastal arc as the Rocky Mountains are related to the Pacific coast ranges." Further, they observed that the volcanoes associated with the Aleutian Islands persist northeastward onto the continent along the Alaska Peninsula, accompanied by shocks of 100 km depth and more. Benioff (1954) noted that earthquake foci in the Aleutians dipped northward under the arc and attributed the mechanism to a complex reverse fault. These fundamental observations of a dipping seismic zone under the Aleutian arc with related shallow seismicity in the Alaska interior are still valid. St. Amand (1957) published a broad review and discussion of Alaska tectonics and applied the term "Denali Fault" to the great structural feature which arcs through the Alaska Range and which had been previously recognized in several separate areas as a major fault. St. Amand also pointed out that the Aleutian trench split just west of

Kodiak with the deepwater part branching toward the east while the other part went through Shelikof Strait, Cook Inlet, and the Susitna depression (Figures 1 and 4). The implication of this is that the Alaska Range southwest of the "McKinley Corner"* belongs structurally to the Aleutian arc. St. Amand speculated that the former trend of the arc was through Kodiak Island and the Kenai Peninsula to the Denali fault near Mt. Hayes while the present trend is along the Aleutian Range to Mt. McKinley. Counterclockwise rotation of the northeast Pacific basin about a pole in the Gulf of Alaska was presented as a possible explanation for this shift in trend. It is interesting to note that relative movements observed and implied by St. Amand in southcentral Alaska are quite similar to the plate motions recently proposed by Grow and Atwater (1970).

Locating the northern terminus of the Benioff zone in Alaska has received little attention, although several authors have commented that the intermediate depth events do not extend far inland. Tobin and Sykes (1966) observed that the intermediate depth earthquakes extended up the Alaska Peninsula 250 km beyond the volcanoes to the vicinity of Mount McKinley, and their map has some events plotted just north of the Denali fault. Tarr (1970) also showed that intermediate depth events occurred just north of the Denali fault, but neither of the latter papers focused much attention on these events. Data presented in this paper define the northern terminus of the Benioff zone.

Numerous authors have studied focal mechanisms of Aleutian arc earthquakes and the evidence for under-thrusting of the Pacific Plate in a

---

*We use this phrase to denote the region of the great structural bend in Alaska in the vicinity of Mt. McKinley.

Cross sections showing the distribution of hypocenters were constructed by projecting all the events in a given rectilinear volume onto a vertical plane. The volumes used were 600 km in length, 300 km deep and 25 or 50 km thick, depending on the density of events in a given region. Earthquakes used in these cross sections were limited to those which had a computed magnitude of 2.0 or greater and an rms travel time residual of 1.0 second or less. A number of events were selected on the basis of magnitude, station distribution and depth control for processing by a modified version of the program HYPO 71 (Lee and Lahr, 1972) and some of the results are shown as section A7 of Figure 2. The solutions for the events which are depicted in section A7 are probably of a better quality than many of the others. In any case, the overall picture remains unchanged.

Examination of the cross sections reveals a dipping zone of activity that is often quite well defined and in some areas exhibits a tendency toward dipping shallowly down to the 50 km level and then more steeply below that - similar to a distinct change in dip found in the central Aleutians by Engdahl (1971, 1973).

The dipping zone of activity in these cross sections is generally 80-100 km thick, in rough agreement with the model proposed by Jacob (1972) and with the observations of Engdahl (1971) for the central Aleutian arc. Refinement of locations by modeling and ray tracing will probably narrow this zone to some degree. Lahr and Page (1972) and Engdahl (1973) have found the Benioff zone to be approximately 10 km thick in lower Cook Inlet and the Central Aleutians, respectively.

Several sets of cross sections parallel to and perpendicular to the Aleutian Range and the Alaska Range (Figures 2A and 2B) show that the Benioff zone continues up the Aleutian Range to a point 75 km north of

northwesterly direction is overwhelming. As more data have been collected, the simplistic picture of a smooth, circular arc with a diameter of some 760 miles (Murray, 1945) has given way to that of a segmental arc composed of relatively short straight lines (West, 1951) meeting at slight angles to one another. These blocks appear to be tectonically independent and they are separated by apparently permanent boundaries (Jordan et al., 1965, and Stauder, 1972). These boundaries have been shown to coincide with the intersections of major transverse tectonic features (Sykes, 1971). There is also a tendency for the main shock of an earthquake sequence in a block to occur near one end, and for the aftershock zone to include the entire segment (Kelleher, 1970; Sykes, 1971). St. Amand (1957) noted that the maximum energy release in the Aleutians seemed to be at junctures of the various blocks composing the arc.

DATA ANALYSIS AND INTERPRETATION

The foci used in this study were determined from data collected from stations of the seismograph network operated by the Geophysical Institute, University of Alaska, and from selected stations of the NOAA Palmer Seismological Observatory which were recorded directly at the University of Alaska. Additional P-wave arrival times obtained from NOAA/Palmer for other NOAA stations not recorded at the University of Alaska were included for events of magnitude larger than about 3. Hypocenters (with the exception of those shown in Fig.2, Section A7, see below) were calculated by a least-square procedure based on P-wave tables compiled by Herrin (1968). Depths were constrained to levels in the Herrin tables and no attempt was made to incorporate corrections for anomalies which may be present due to the complex and largely unknown geologic structure of central Alaska. Accuracy of epicenters is difficult to determine precisely, but all indications are that they are within 10 km of their true positions (VanWormer et al., 1973).

the Denali fault where the zone abruptly terminates near the northern foothills of the Alaska Range at about 64.25°N (Figure 2A5). This transection of the Denali fault by the Benioff zone casts doubt on the interpretation of the Denali as a simple surface expression of the transform boundary between the Pacific plate and the continent analogous to the San Andreas fault in California. Also, the extension of the Denali fault system to the west of Mt. McKinley is difficult to explain in this context. On the other hand, it is inconceivable that such a large, recently active fault does not play an important tectonic role in the region of the McKinley corner. The nature of this role is not clear at this time.

The geometry of the dipping focal zone as determined from some 60 cross sections is illustrated by the contour map of its upper surface shown in Figure 3. The Benioff zone is quite well defined in this manner except in the vicinity of the Yentna River where a relative paucity of hypocenters leads to nebulous interpretation of cross sections (Figure 2A6). The shape of the zone in this region is indeterminate from the hypocenter data alone. North of the Yentna River the zone dips more steeply (∿63°) and strikes N45°E whereas south of the river it dips less steeply (∿56°) and strikes more northerly (N13°E).

We interpret this anomalous area to be a break in the structure similar to the break near Amchitka Pass between the Rat Island block and the Delarof Island block (Stauder, 1972). Although the various other observations listed below do not individually suggest this relationship as strongly as the hypocenter information, when taken together they lend support to interpreting this kink in the zone as a block juncture.

Examination of a topographic map (or see Figure 4) shows that the Yentna River is at a bend in the mountains and that the width of the massif south of the river is approximately twice the width of the massif northeast of the river. Gravity data for this area (Woollard et al., 1960) indicate a deep-seated change in trend in this area, as does the termination of the volcano chain at Mt. Spurr 100 km southwest of the Yentna River. There is also a noticeable decline in seismic activity (Figure 2A6) within the Benioff zone in the vicinity of the Yentna River.

Aftershocks of the great 1964 Alaska earthquake were confined southwest of an extension of the line of the Yentna River anomaly (Page 1968; Algermissen et al., 1972). This line, when extended even further southeast, coincides with the continental shelf break in the Cape Yakataga area.

The initial shock in 1964 was very near the northeast terminus of the aftershock zone. The pattern of a main shock near one end of a block is often observed in the Aleutian arc farther to the west where the tectonic setting is much simpler (Kelleher et al., 1973). The 3 November 1943 magnitude 7.3 earthquake also occurred near the Yentna River line and may be further evidence of a fundamental structural break. It is interesting to note that in historic time no large earthquakes have occurred between the Yentna River line and the Alaska Range to the north and northeast (Davis and Echols, 1962).

Earthquake magnitudes determined by the Geophysical Institute are generally higher for most of Alaska than those reported by the NOAA Palmer Observatory. Nine of eleven exceptions to this generalization for a randomly selected two month period occurred in the region bounded

on the north by the terminus of the Benioff zone and on the south by the Yentna River (VanWormer et al., 1973). We hypothesize that the relatively larger magnitudes NOAA computed for this area are due to very low attenuation of body waves traveling upward along the dipping zone to the NOAA station at Palmer. A similar situation of very low attenuation of amplitude was reported for waves traveling up-dip in the Tonga-Kermadec arc by Oliver and Isacks (1967).

It is clear from the above observations of topography, gravity, volcanoes, aftershocks, magnitudes, and particularly hypocenter distributions that there is some structural anomaly at depth in the Yentna River region.

CONCLUSIONS

Our interpretation of the tectonics in southcentral Alaska is schematically represented in Figure 5. We propose that there are two blocks which are similar in character to the blocks composing the western Aleutian arc. The boundary between these blocks extends from the Yentna River through Prince William Sound, perhaps as far as the continental shelf break near Yakutat Bay. The northern, or McKinley block, extends northwest beyond the Denali fault to the northern edge of the Alaska Range massif and dips more steeply than the adjacent Kenai block. The southwest boundary of the Kenai block is not presently known but we speculate that it may be at the bend in the volcano line in Kamishak Bay, although the 1964 aftershocks indicate the boundary may be near the southwest end of Kodiak Island. The evidence presented here and by Davies and Berg (1973) indicates that the subduction zone in the eastern Aleutian Arc is the Shelikof Strait - Cook Inlet - Susitna River topographic low and is not offshore in the trench area east of Kodiak Island. The

continental material between the abyssal plain and the subduction zone is hypothesized to be a "raft" of material riding on the Pacific plate. We speculate that the great 1964 earthquake, a shallow thrust mechanism (e.g. Plafker, 1965), was a result of continued underthrusting of the Pacific plate beneath the rafted continental material of the Kenai block.

ACKNOWLEDGEMENTS

We express our thanks to Dr. D. B. Stone who critically reviewed the manuscript. This study was funded by the State of Alaska, by the Advanced Research Projects Agency of the Department of Denfense (monitored by the Air Force Office of Scientific Research under contract F44620-73-C-0053), and the National Aeronautics and Space Administration contract NAS 5-21833.

REFERENCES

Algermissen, S. T., W. A. Rinehart, R. W. Sherburne and W. H. Dillinger, Jr. (1972). Preshocks and aftershocks, in The Great Alaska Earthquake of 1964: Seismology and Geodesy, Vol. 2, Nat. Acad. Sci., Wash. D. C., 313-364.

Benioff, H. (1954). Orogenesis and deep crustal structure-additional evidence from seismology, Geol. Soc. Am., 65, 385-400.

Davies, J. and E. Berg (1973). Crustal morphology and plate tectonics in south central Alaska, Bull. Seism. Soc. Am., 63, 673-677.

Davis, T. Neil, and C. Echols (1962). A table of Alaskan earthquakes, 1788-1961, Geophysical Research Report No. 8, University of Alaska, Fairbanks, Alaska.

Engdahl, E. R. (1971). Explosion effects and earthquakes in the Amchitka Island region, Science, 173, 1232-1235.

Engdahl, E. R. (1973). Relocation of intermediate depth earthquakes in the central Aleutians by seismic ray tracing, Nature Phys. Sci., 245, 23-25.

Grow, J. A. and T. Atwater (1970). Mid-Tertiary tectonic transition in the Aleutian Arc, Geol. Soc. Am., 81, 3715-3722.

Gutenberg, B. and C. F. Richter (1954). Seismicity of the Earth and Associated Phenomena, Princeton University Press, Princeton, New Jersey, p. 32.

Herrin, E. (chairman) (1968). 1968 Seismological tables for P phases, Bull. Seism. Soc. Am., 58, 1196-1211.

Jacob, K. H. (1972). Global tectonic implications of anmalous seismic P traveltimes from the nuclear explosion "Longshot", J. Geophys. Res., 77, 2556-2573.

Jordan, J. N., R. A. Black and J. F. Lander (1965). Aftershocks of the 4 February 1965 Rat Island Earthquake, Science, 148, 1323-1325.

Kelleher, J., L. Sykes, J. Oliver (1973). Possible criteria for predicting earthquake locations and their application to major plate boundaries of the Pacific and the Caribbean, J. Geophys. Res., 78, 2547-2585.

Kelleher, J. A. (1970). Space-time seismicity of the Alaska-Aleutian seismic zone, J. Geophys. Res., 75, 5745-5756.

Lahr, J. C. and R. A. Page (1972). Hypocentral locations in the Cook Inlet region of Alaska, Abstract in EOS, 53, 1042.

Lee, W. H. K., and J. C. Lahr (1972). HYPO71: a computer program for determining hypocenter, magnitude, and first motion pattern of local earthquakes, US Geological Survey, Open-file Report. 100 p.

Murray, H. W. (1945). Profiles of the Aleutian Trench, Geol. Soc. Am., 56, 757-782.

Oliver, J. and B. Isacks (1967). Deep Earthquake zones, anomalous structures in the upper mantle, and the lithosphere, J. Geophys. Res., 72, 4259-4275.

Page, R. (1968). Aftershocks and microaftershocks of the great Alaska earthquake of 1964, Bull. Seism. Soc. Am., 58, 1131-1168.

Plafker, G. (1965). Tectonic deformation associated with the 1964 Alaska earthquake, Science, 148, 1675-1687.

St. Amand, P. (1957). Geological and geophysical synthesis of the tectonics of portions of British columbia, the Yukon Terriory, and Alaska, Geol. Soc. Am., 68, 1343-1370.

Stauder, W. (1972). Fault motion and spatially bounded character of earthquakes in Amchitka Pass and the Delarof Islands, J. Geophys. Res., 77. 2072-2080.

Sykes, L. R. (1971). Aftershock zones of great earthquakes, seismicity gaps, and earthquake prediction for Alaska and the Aleutians, J. Geophys. Res., 76, 8021-8041.

Tarr, A. C. (1970). New Maps of Polar Seismicity, Bull. Seism. Soc. Am., 60, 1745-1757.

Tobin, D. G. and L. R. Sykes (1966). Relations of hypocenters of earthquakes to the geology of Alaska, J. Geophys. Res., 71, 1659-1668.

VanWormer, D., J. Davies and L. Cedney (1973). Central Alaska earthquakes during 1972, Sci. Rept. UAG R-224 Geophysical Institute, University of Alaska, Fairbanks, Alaska.

West, S. S. (1951). Major shear fractures of Alaska and adjacent regions, Trans. Am. Geophys. Union, 32, 81-96.

Woollard, G. P., N. A. Ostenso, E. Thiel, and W. E. Bonini (1960). Gravity anomalies, crustal structure, and geology in Alaska, J. Geophys. Res., 65, 1021-1037.

Figure Captions

Figure 1. Location map of Alaska showing major features referenced in text.

Figure 2A. Cross sections through the Benioff zone. Note that the vertical exaggeration is 2:1 in all sections. Sections A1-A6 are 50 km thick perpendicular to the plane of the figure. Section A7, 500 km thick perpendicular to the plane of the figure, illustrates the clarity of the dipping zone when strict quality control is applied to the data. Locations and look directions of the cross sections are shown in the accompanying maps. Note the abrupt termination of the Benioff zone to the left (north) in section A6.

Figure 2B. Cross sections of the northern part of the Benioff zone. These sections are 25 km thick perpendicular to the plane of the figure and are nearly along the strike of the zone. Locations and look directions are shown in the accompanying map. Sections A1-A6 and B1-B8 are representative of the more than 60 cross sections analyzed in this study.

Figure 3. Contours of the upper surface of the Benioff zone as determined in this study. Contour interval is 50 km. Southwest termination of the contours represents only the arbitrary limit of hypocenter selection. Northeast termination of contours represents real termination of the Benioff zone. The star is the epicenter of the 1964 earthquake and the solid circle isthe epicenter of the 1943 magnitude 7.3 earthquake (as relocated by Sykes, 1971).

Figure 4. Mosaic of 19 Earth Resources Technology Satellite (ERTS-1) images. Images were obtained in early November, 1972. The sun is illuminating the area from the lower right. The Denali fault arcs across the scene from upper right to center left.

Figure 5. Diagrammatic representation of the subducting Pacific plate in south central Alaska as interpreted in this study. Circle and star are as in Figure 3. As stated in the text, the precise nature of the Benioff zone at the Yentna lineament is not clearly defined. Thus the depth contours in the figure are broken at the bend in the zone.

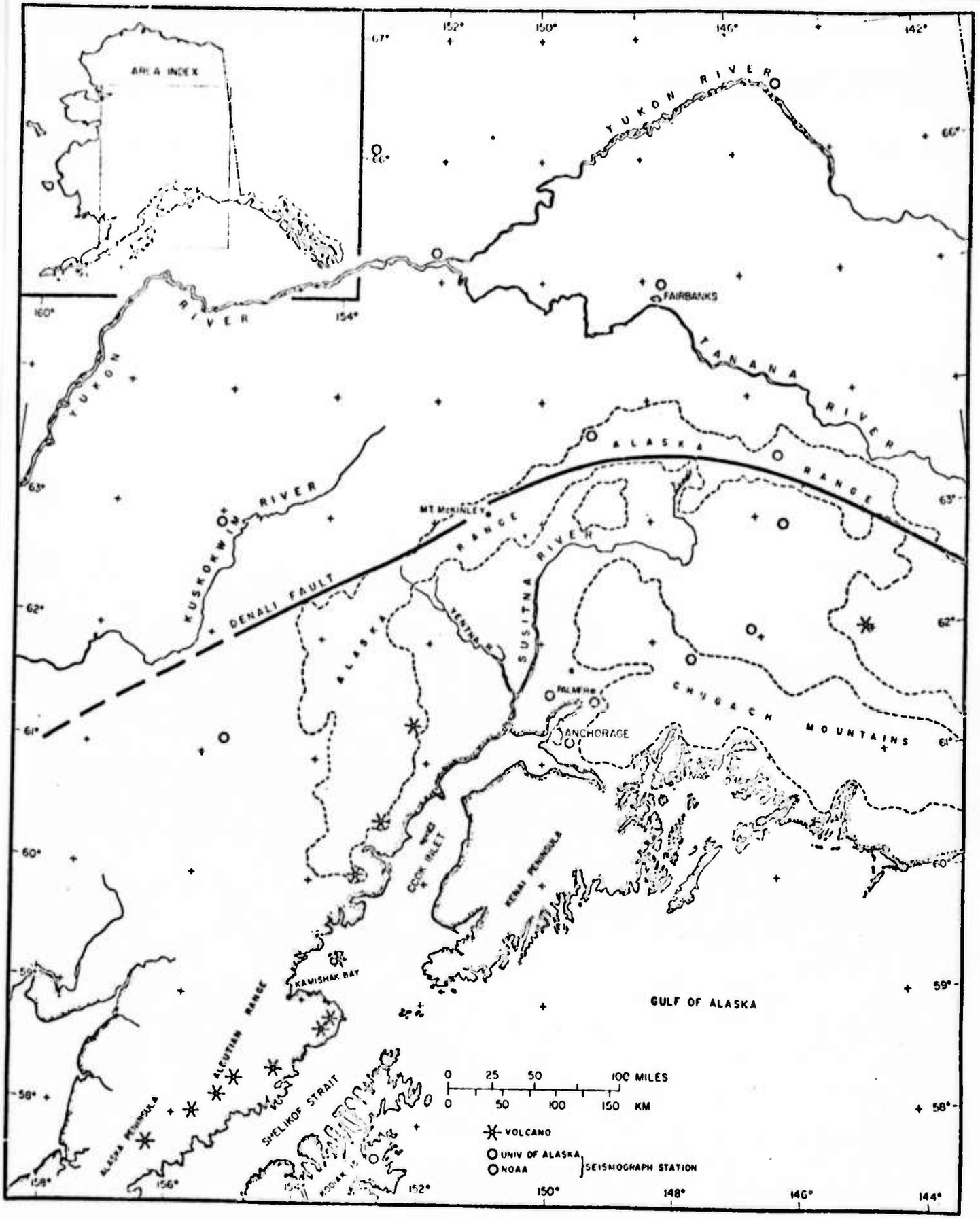

Figure 1. Location map of Alaska showing major features referenced in text.

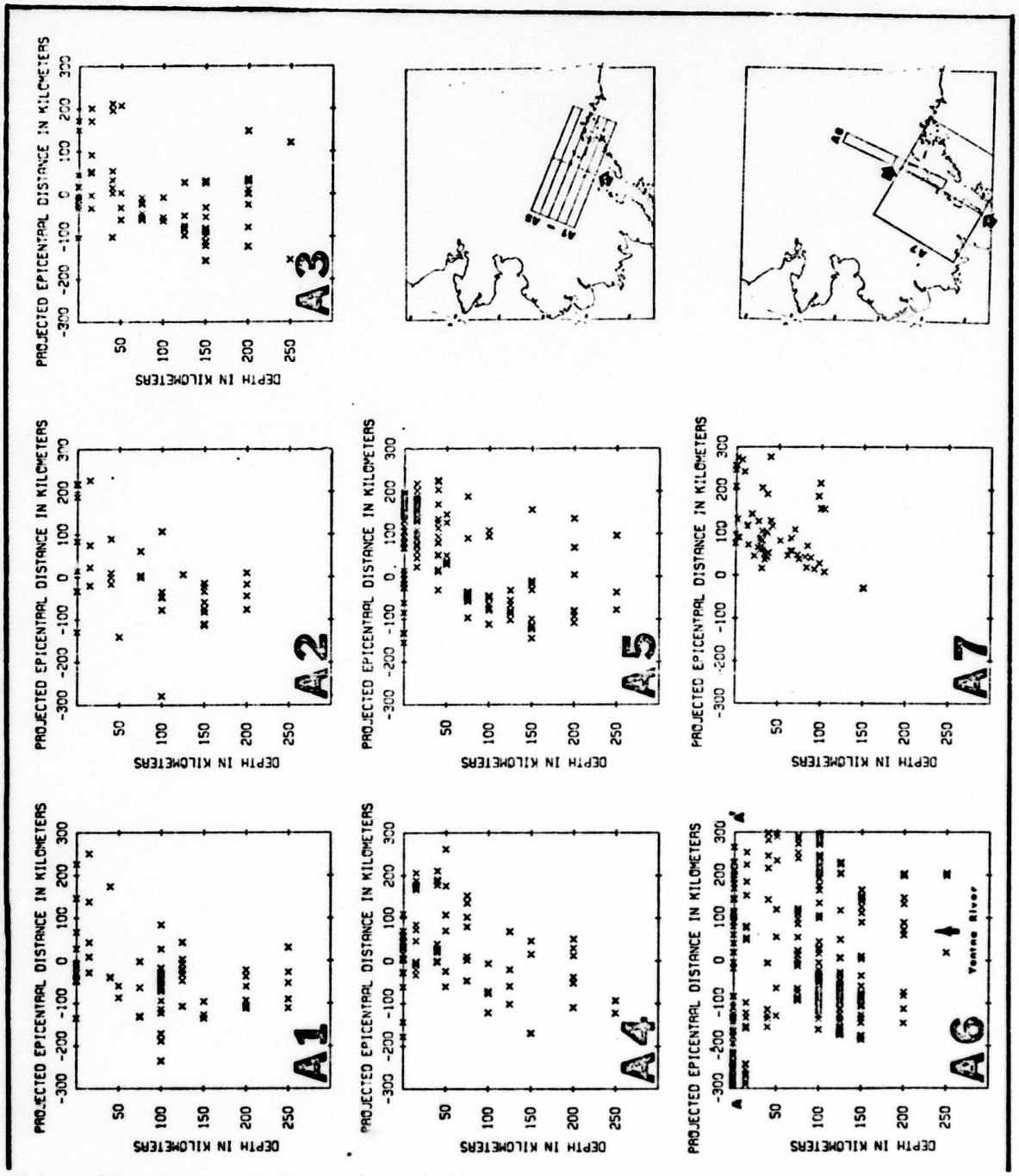

Figure 2A. Cross sections through the Benioff zone. Note that the vertical exaggeration is 2:1 in all sections. Sections A1-A6 are 50 km thick perpendicular to the plane of the figure. Section A7, 500 km thick perpendicular to the plane of the figure, illustrates the clarity of the dipping zone when strict quality control is applied to the data. Locations and look directions of the cross sections are shown in the accompanying maps. Note the abrupt termination of the Benioff zone to the left (north) in section A6.

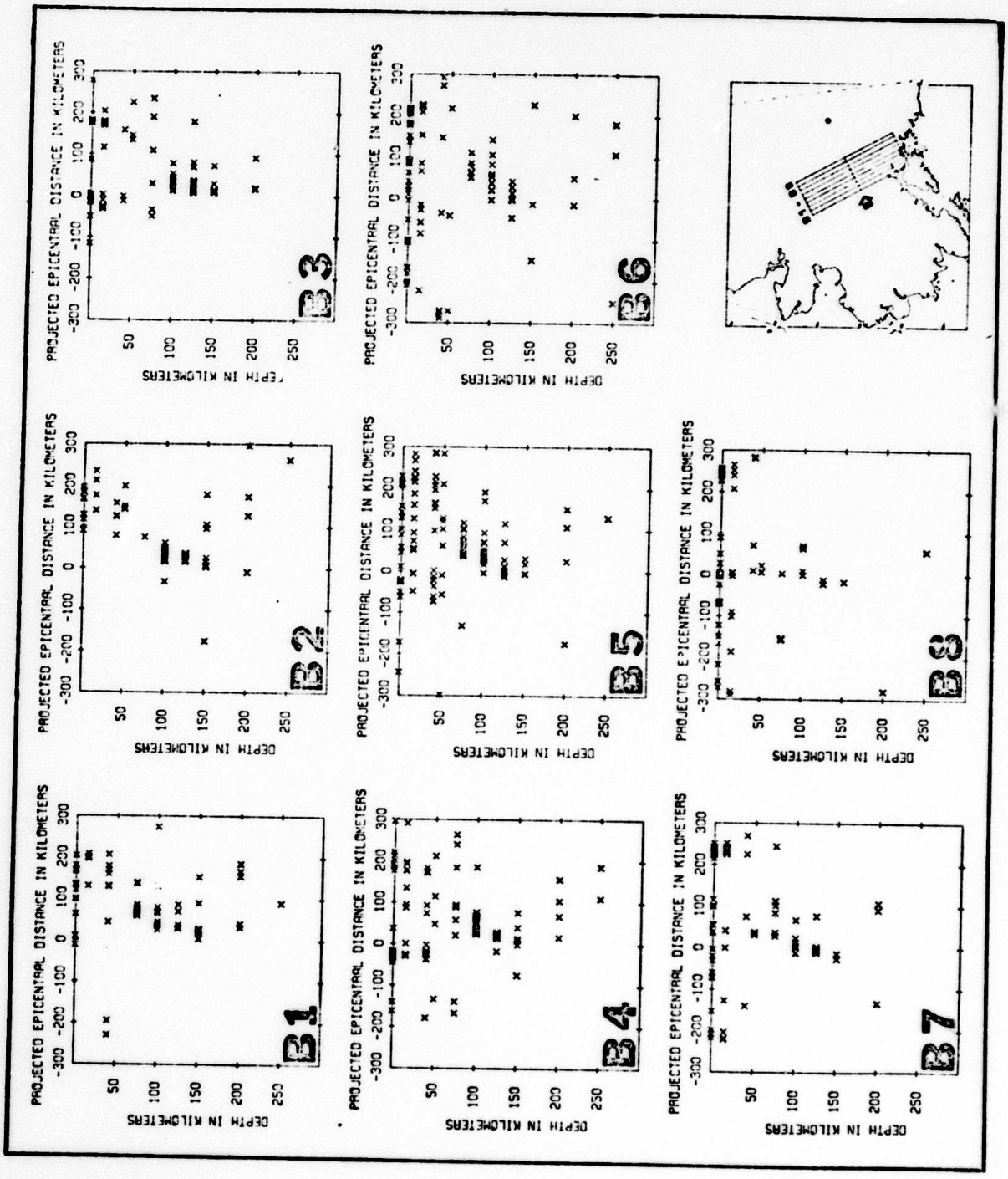

Figure 2B. Cross sections of the northern part of the Benioff zone. These sections are 25 km thick perpendicular to the plane of the figure and are nearly along the strike of the zone. Locations and look directions are shown in the accompanying map. Sections A1-A6 and B1-B8 are representative of the more than 60 cross sections analyzed in this study.

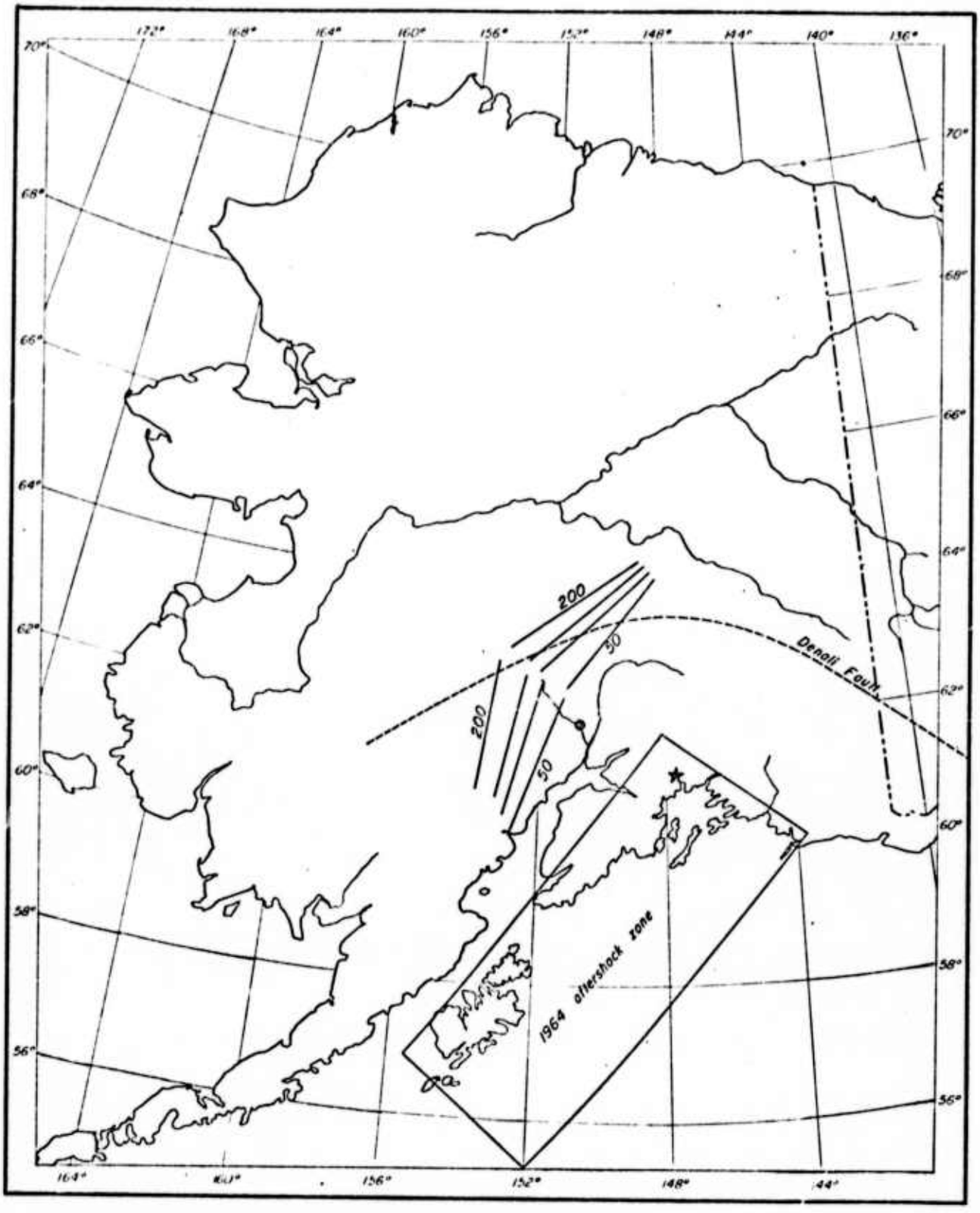

Figure 3. Contours of the upper surface of the Benioff zone as determined in this study. Contour interval is 50 km. Southwest termination of the contours represents only the arbitrary limit of hypocenter selection. Northeast termination of contours represents real termination of the Benioff zone. The star is the epicenter of the 1964 earthquake and the solid circle isthe epicenter of the 1943 magnitude 7.3 earthquake (as relocated by Sykes, 1971).

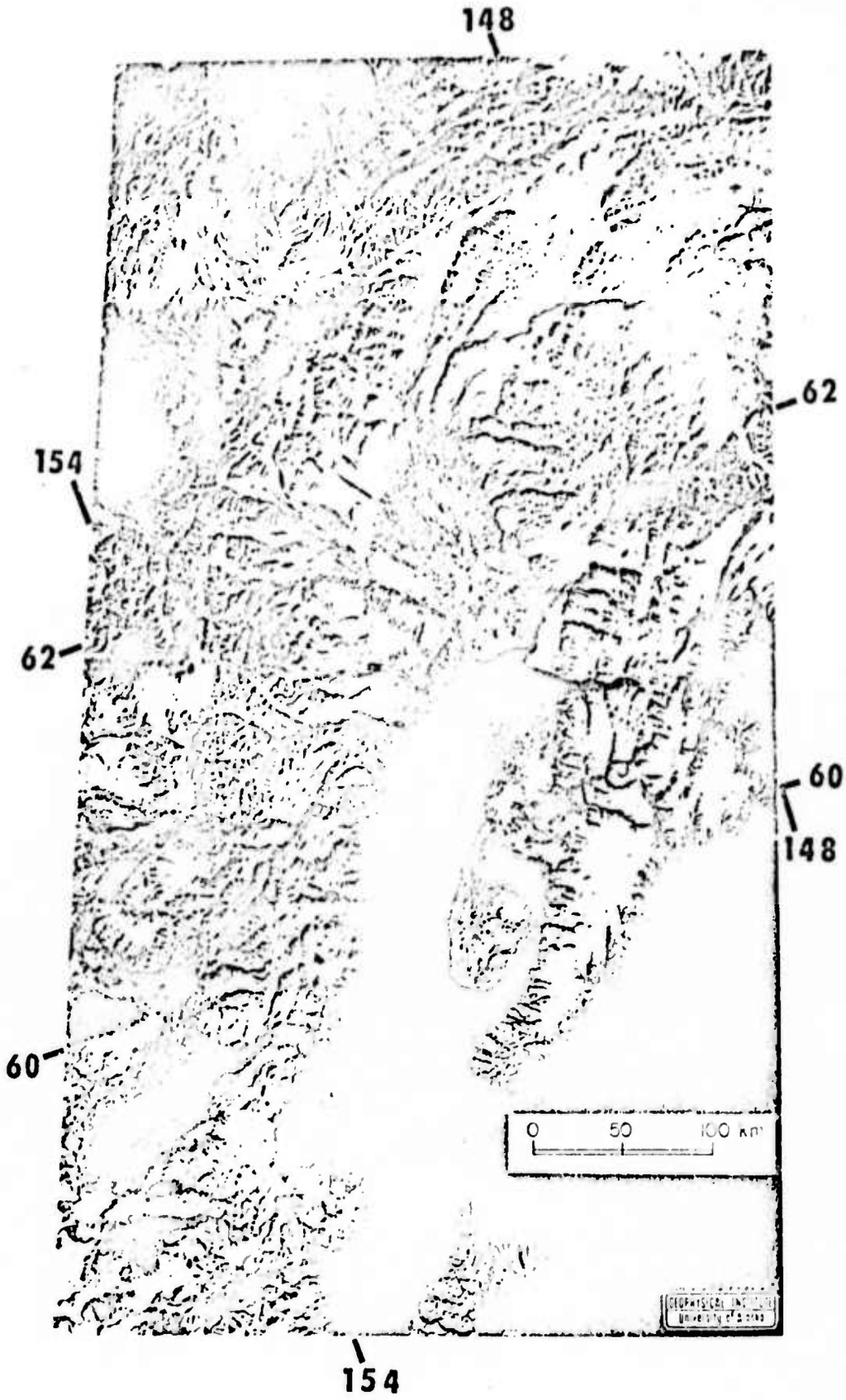

Figure 4. Mosaic of 19 Earth Resources Technology Satellite (ERTS-1) images. Images were obtained in early November, 1972. The sun is illuminating the area from the lower right. The Denali fault arcs across the scene from upper right to center left.

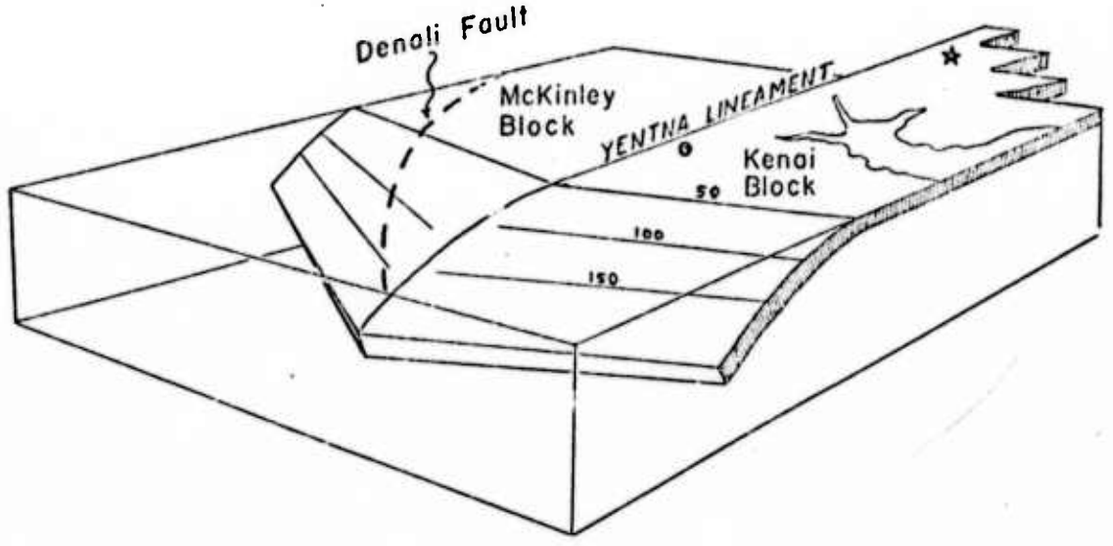

Figure 5. Diagrammatic representation of the subducting Pacific plate in south central Alaska as interpreted in this study. Circle and star are as in Figure 3. As stated in the text, the precise nature of the Benioff zone at the Yentna lineament is not clearly defined. Thus the depth contours in the figure are broken at the bend in the zone.

3. Source Mechanics for Small Magnitude Earthquakes in Central Alaska

by B. Bhattacharya and N. N. Biswas

ABSTRACT

P-wave first-motion for 41 selected earthquakes ($3.0 \leq m_b \leq 5.5$) located in central and southcentral Alaska have been studied. The events with focal depths less than 60 km show either strike-slip or normal faulting focal mechanism. The events with focal depths greather than the above value show nearly pure dip-slip motions. The solutions in general show a northwest-southeast orientation of the pressure axes, a feature in good agreement with that predicted from North Pacific plate tectonics.

INTRODUCTION

The Anchorage earthquake of 1964 led to more research aimed at understanding the seismotectonic setting of the Alaska-Aleutian region. Some of the important results revealed by the ensuing studies and which are pertinent to the present investigation have been discussed by Stauder (1968a,b). From the first-motion solutions, Stauder demonstrated a close correlation between the nature of motions on active faults along the coastal belt of central Alaska and Aleutian regions and those predicted from the hypothesis of global tectonics for the above regions.

Relationships between fault-plane solutions and regional tectonics in central Alaska have been investigated by Gedney and Berg (1969a,b). Gedney (1970) integrated earlier fault-plane solutions with those from small magnitude earthquakes located from Kodiak Island to the Alaska Range along a NNE-SSW line through Cook Inlet. For a number of events, he obtained a northwest-southeast trending pressure axis, a feature which is in agreement with the results obtained for the coastal belt of central Alaska by Stauder and Bollinger (1966) and Stauder (1968b).

On the north of the Alaska Range, fault plane solutions for two shallow moderate size earthquakes and their aftershock sequences have been discussed by Jordan et al. (1968), Gedney and Berg (1969) and Gedney (1970). The first event was located about 100 miles west of Fairbanks and showed a left-lateral movement along a north-south trending steeply-dipping fault. The second event was located just south of Fairbanks and occurred along a northwest-southeast trending fault; the motion had equal components of right-lateral strike-slip and normal faulting.

Biswas (1973), from P-wave travel time residual studies, inferred the inland continuation of the Aleutian-Alaska Peninsula underthrust lithospheric plate under southcentral and central Alaska. As incorporated in Section 2 of this report, Van Wormer et al. (1974) have demonstrated the termination of the above feature some 75 km north of the Denali fault. Lahr (1974), in addition to obtaining similar results, has related the fault plane solutions in Cook Inlet to the geometry of the plate from improved seismic coverage around the above area. He obtained a N28°E striking Benioff zone with a dip of about 45°-50°; the plate was shown to reach a depth of about 150 km from the surface. Lahr showed also that the earthquakes at intermediate depths (> 60km) are characterized by nearly pure dip-slip motions with the tension axis oriented downdip along the seismic zone.

In the present study, we have examined the source mechanisms of small magnitude earthquakes in central and southcentral Alaska with respect to the current knowledge of the North Pacific plate tectonics.

DATA

We have analyzed short period records for the entire year of 1973 obtained by the central Alaskan seismic networks (Geophysical Institute and NOAA). The correct polarity of the seismograph at each station was checked by studying the sense of motion from a presumed underground explosion (12 September 1973, m_b = 6.8) in Novaya Zamlaya.

Out of the total of 108 events located in the area of interest, P-wave first motions for 41 events could be read at most of the stations with certainty. The locations and origin times for these events were

noted from NOAA's Monthly Bulletin (PDE) and are listed in Tables 1 and 2; the magnitudes of the earthquakes vary from 3.0 to 5.5. The locations of the stations and epicenters of the events considered are shown in Figure 1.

To determine the emergence angle at the focus for each earthquake, a plane layered crust-upper mantle P-wave velocity structure (Table 4) has been constructed from the results discussed in Section 1 of this report. Since we cannot characterize the P_g crustal phase yet, P-wave velocity for the first crustal layer has been taken from Hales and Asada (1966). Although this value for the P_g phase is appropriate for southcentral and southeastern Alaska, we do not anticipate any significant errors in using the above P_g value for all of central Alaska in computing the angle of emergence.

The computations of the emergence angles have been performed by the HYPO-71 (Lee and Lahr, 1972) computer program. For most of the events, the combination of short epicentral distance and intermediate focal depth yielded the first arrivals as direct waves. Due to this fact, we have represented the first-motion dilatations and compressions on an equal area projection (10 cm Schmidt net) of the upper hemisphere. For those cases where the first arrivals were refracted, the representation on the upper hemisphere has been retained for consistency.

RESULTS

The representation on the stereo-net of the distribution of compressions and dilatations of first-motions for each event was visually best-fitted to a nodal plane. A second nodal plane, orthogonal to the first, was then drawn as a best-fit through the data points. This

procedure was applied to the data for all the 41 earthquakes; the results have been divided into two groups on the basis of focal depth and the nature of the solution, that is, dip-slip or other type, the discussion of which follows.

The earthquakes listed in Table 1 have hypocenters located either in the crust or 10 to 15 km deeper than the average depth of the M-discontinuity ($\sim$ 45 km) in central Alaska (Table 4). These have been placed in one group. Their first motion solutions are shown in Figures 2 and 3, which show either strike-slip or normal faultings. The hypocenters of the earthquakes listed in Table 2 vary in depth from 64 to 171 km, with one exception (event No. 20), for which it is 32 km. However, for the majority of the events, the focal depths exceed 100 km. The first-motion solutions of all these events show nearly pure dip-slip motions as shown in Figures 4 and 5. These solutions have been placed in the second group.

In Tables 1 and 2 we have also shown the values of the dip direction, dip and slip angle (angle measured in the nodal plane between the horizontal and the direction of motion, if the nodal plane in question be considered as the fault-plane) for each of the nodal planes and the trend and the plunge of the B, P and T axes. The B axis is the null axis, i.e. the intersection of the two nodal planes. The P and T axes are the axes of greatest and least compressive stresses, respectively. Of the two nodal planes, plane 1 refers to the one which has relatively greater dip value.

In Figures 6 and 7 the first-motion solutions of the first and second groups of events, respectively, have been shown in relation to

the major structural trends in central Alaska. These include seven prominent arcuate fault systems with right lateral motions, except the faults shown by barbed lines along the coast which are thrust type. The shaded and non-shaded sections in the mechanism diagrams represent the dilatational and compressional areas, respectively. The trend of the pressure axis for each case is shown by a solid arrow.

Six of the events (Nos. 1, 8, 10, 11, 14 and 18) of the first group represent strike-slip motion (Figure 6); one of the nodal plane strikes approximately in the east-west direction, while the other in the north-south direction and both of them dip steeply by more than 80°. The pressure axes are nearly horizontal ($1° \leq$ plunge $\leq 8°$, Table 1) and are oriented either in the southeast-northwest (Nos. 8, 10, 11, 18) or in the northeast-southwest (Nos. 1, 14) direction.

Three (Nos. 1, 11 and 18) of the strike-slip events are located in the vicinity of the faults marked H, C and G (Figure 6). On the basis of the orientation of the fault traces, we interpreted the east-west striking nodal plane as the fault-plane for these events. The remaining three events (Nos. 8, 10 and 14) are located in valleys having thick sedimentary deposits with no exposed fault traces. Thus we have not identified which of the two nodal planes is the fault plane for these cases.

The first-motion solutions for the remaining twelve earthquakes of the first group represent normal faulting. Except for Nos. 2 and 7, the events show the dip of the two nodal planes in the range of 30° to 60°. For the two former events, the dip increases to 69° to 71°. The plunge of the tension axis has been found to vary from 0° to 28°.

Moreover, for six of the events (Nos. 4, 9, 12, 13, 15, 17) the two nodal planes strike approximately in the northwest-southeast direction whereas four of them (Nos. 2, 3, 5 and 6) show about northeast-southwest and two (Nos. 7 and 16) show approximately east-west striking nodal planes.

The earthquakes of the second group are all located in southcentral Alaska (Figure 7). The first-motion solutions for these events correspond to underthrust type of motion, that is, the foot wall is sliding downward with respect to the hanging wall. Also, the direction of the dip of one of the nodal planes varies from west to northwest while that of the other varies from east to southeast. Exception to these general dip directions were obtained for Nos. 5, 6, 13, 17, 21 and 23. For these cases, one of the nodal planes dips either in the south or southwest direction while the other in the north and northeast direction. The trend of the nodal planes for event No. 8 does not belong to either of the above two types; one of the nodal planes dips in the NNE direction, the other in the SSW direction.

The values of the dip for both the nodal planes range from 30° to 60° except for events No. 1, 16, 22, for which it is less than 30°. Also the plunge of the tension axis varies from 68° to 88°, except for events No. 1 and 8. For these two cases, the values are 53° and 46°, respectively. The plunge of the pressure axis varies from 0° to 22° except for event No. 1, for which it is 37°.

DISCUSSION

Although the extension of the North Pacific lithospheric plate across the Denali fault to central Alaska up to at least 63°N has been suggested (Van Wormer et al., 1974; Lahr, 1974), the relationships between

the sources of high seismicity, particularly from the Denali fault to about 66°N, and the plate motion are difficult to resolve due to the complicated structural setting of the above section of central Alaska (Figure 6). However, to derive a regional pattern from the individual first-motion solutions, we have prepared composite diagrams for the strike-slip and normal faults separately for events located north of the Denali fault. Figure 8a shows such a solution for the strike-slip faults revealed by event Nos. 8, 10, 11, 14 and 18.

In the above figure, two nodal planes, one striking approximately east-west and the other north-south, give a visual best-fit to the data. If the former nodal plane is chosen as the regional orientation of the strike-slip faults, then the solution will imply a right-lateral motion on a nearly vertical fault with pressure axis oriented in the northwest-southeast direction.

Figure 8b shows the composite solution of normal faults for earthquakes Nos. 4, 9, 12, 13 and 15. Data for two of the events (Nos. 5 and 7) have been excluded from the above figure due to grossly different strike directions of their nodal planes compared to others. This does not imply that the first motion solutions for these two events are inaccurate, rather the orientation of their fault planes does not follow the regional trend, a feature not uncommon for a complicated active tectonic area.

The above composite solution (Figure 8b) shows a steeply dipping northwest-southeast orientation of the pressure axis, which is in close agreement with that obtained for the strike-slip faults. The visual best-fit of the data with two nodal planes has uncertainties which are equivalent to errors from $\pm$ 5° to $\pm$ 10° in the dips and strikes of the nodal planes.

The first-motion solutions of the intermediate depth earthquakes in southcentral Alaska have a general characteristic of underthrusting, i.e. nearly pure dip-slip motions, as mentioned before. In addition, if the northwest dipping nodal plane is interpreted as the fault plane, the focal model for most of the events will correspond to an average plunge of 75° for the tension axis. These features imply a downward sliding of the foot wall with respect to the hanging wall, a result in close agreement with those obtained by Lahr (1974) in the Cook Inlet area.

CONCLUSIONS

In view of the current knowledge of the North Pacific plate tectonics in central Alaska, we may infer that the shallow earthquakes occurring in the above area due to a direct consequence of the bending of the underthrusting lithospheric plate, most likely will be associated with normal faulting. If the stored strain energy is released on the pre-existing faults, the above pattern may change to strike-slip motions. On the other hand, the source mechanism of earthquakes with intermediate focal depth (> 60km), resulting from the sinking of the lithospheric plate under its own weight (Le Pichon et al., 1973) will be associated with nearly pure underthrusting motions. This implies downdip orientation of the tension axes along the seismic zone. If the rupture plane parallels the dip of the seismic zone, the tension axes will be at an angle ($\sim$ 45°) to the plate boundary. For small magnitude earthquakes, whether the rupture plane will always be parallel to the plate boundary or not seems to be an open question.

The results of the present study for earthquakes with focal depth less than 60 km in central Alaska are in general agreement with the

observations for the causes of shallow events made above. However, we obtained a number of solutions in the above group which do not agree with the major tectonic pattern of the area. Further studies of source mechanism for events located in and around those which yielded inconsistent solutions are needed for a complete understanding of the nature of the stored strain energy release in the area of interest. Such studies are particularly important for areas which are seismically active and at the same time, lie outside the northern limit of the underthrust lithospheric plate in interior Alaska.

The earthquakes with focal depths greater than 60 km are all located in southcentral Alaska where the North Pacific plate tectonics seem to control the seismic activities. The focal mechanism of the above events show good correlation with the features discussed above for an underthrust plate sinking by its own weight.

Event Number	Date 1973	Origin Time Hr	Min	Sec	Depth (km)	Lat (°N)	Long(°W)	Plane 1 Dip Dir. (deg.)	Plane 1 Dip (deg.)	Plane 1 Slip Ang. (deg.)	Plane 2 Dip Dir. (deg.)	Plane 2 Dip (deg.)	Plane 2 Slip Ang. (deg.)	B Trend (deg.)	B Plunge (deg.)	P Trend (deg.)	P Plunge (deg.)	T Tren (deg.)	T Plunge (deg.)
1	Feb 7	18	52	23.1	45	61.3	150.5	23	86	4	113	86	3	245	85	70	7	157	0
2	Feb 8	15	00	48.9	54	61.8	150.2	353	69	77	141	24	59	258	12	14	63	163	24
3	Feb 9	14	09	53.1	34	62.3	150.7	303	49	86	129	40	82	37	4	278	82	125	6
4	Feb 28	19	03	51.2	39	65.6	150.0	214	59	83	49	31	80	307	5	195	74	40	16
5	Mar 21	05	40	37.9	18	64.8	147.8	139	50	86	315	40	84	47	3	171	87	317	5
6	Mar 28	07	26	33.9	21	64.8	147.5	143	46	76	305	46	76	42	11	221	80	134	0
7	May 7	17	39	45.7	39	65.4	150.0	193	71	86	26	19	81	284	5	185	63	14	28
8	May 23	17	48	59.0	34	64.0	150.7	11	87	4	101	87	4	212	9	325	2	55	4
9	Jun 5	03	37	14.6	38	63.6	150.9	222	60	74	11	34	62	124	15	262	69	31	14
10	Jun 16	07	50	45.2	7	64.7	147.2	90	88	2	180	88	2	325	3	124	3	225	0
11	Jun 17	09	34	41.4	26	65.5	150.2	160	89	1	71	89	1	318	3	114	1	27	0
12	Jun 18	01	49	05.4	29	65.1	147.0	243	40	85	72	40	85	337	6	102	84	68	6
13	Jun 19	16	13	13.3	26	64.8	147.5	242	50	74	86	42	72	342	14	177	78	74	6
14	Jul 4	19	54	30.7	6	64.8	147.5	283	84	5	192	85	7	61	81	237	8	327	0
15	Jul 30	01	06	55.2	19	64.7	149.4	228	58	78	25	32	70	131	11	254	80	40	15
16	Oct 4	01	39	21.9	9	62.7	151.6	14	50	58	149	49	58	262	25	82	66	353	0
17	Nov 20	04	02	58.9	57	62.0	149.0	260	60	85	90	30	81	352	4	246	75	82	14
18	Dec 22	08	41	30.9	16	63.5	151.3	161	88	8	252	82	2	53	83	297	4	206	5

Table 2.
Locations (Lat., Long.), origin times and details of the P-wave first-motion solutions for 23 earthquakes (focal depth > 5) km) considered in this study.

Event Number	Date 1973	Origin Time Hr	Min	Sec				Plane 1			Plane 2			B		P		T	
					Depth (km)	Lat (°N)	Long(°W)	Dip Dir. (deg.)	Dip (deg.)	Slip Ang. (deg.)	Dip Dir. (deg.)	Dip (deg.)	Slip Ang. (deg.)	Trend (deg.)	Plunge (deg.)	Trend (deg.)	Plunge (deg.)	Tren (deg.)	Plunge (deg.)
1	Jan 5	02	24	20.3	105	60.1	153.0	85	83	83	249	6	79	356	3	263	37	86	53
2	Jan 18	21	34	30.5	144	60.1	153.4	77	52	72	289	40	67	178	16	268	8	19	74
3	Feb 4	07	09	12.2	111	63.1	150.8	73	58	65	295	40	57	177	22	271	11	21	68
4	Feb 6	20	29	34.8	134	60.0	152.7	304	59	75	99	33	68	206	12	114	14	336	72
5	Feb 9	09	39	29.9	95	62.1	151.2	66	46	90	246	44	90	155	0	69	0	26	88
6	Feb 16	02	25	23.8	109	63.0	150.6	212	60	90	40	30	90	301	1	31	14	220	78
7	Feb 23	08	10	39.9	64	61.5	150.8	286	46	85	110	44	84	18	3	108	2	264	88
8	Feb 26	19	16	21.7	111	63.1	150.4	118	78	51	13	42	21	219	39	327	22	81	46
9	Feb 27	00	52	29.1	70	61.9	151.0	108	50	33	278	40	81	14	6	283	4	145	83
10	Mar 5	08	30	49.2	106	63.7	148.4	132	48	85	308	48	87	41	2	131	0	297	85
11	Mar 23	16	15	47.1	113	62.6	151.5	330	60	89	148	30	90	61	1	149	14	334	76
12	May 6	10	54	08.4	154	63.2	150.7	232	58	71	24	36	67	133	14	41	12	276	73
13	May 14	22	33	37.4	112	63.8	148.5	119	52	78	283	40	78	23	8	291	8	171	80
14	May 26	23	04	38.0	171	60.2	154.0	134	60	33	302	30	78	41	6	310	14	148	74
15	Jul 30	17	38	34.2	102	63.0	149.8	128	72	82	336	20	68	221	7	314	26	113	64
16	Aug 11	02	40	10.0	120	62.9	150.6	78	52	74	281	42	72	176	12	267	6	20	75
17	Aug 17	21	30	02.3	137	62.9	151.2	241	50	74	35	44	72	139	12	48	6	308	78
18	Aug 19	17	34	51.3	130	63.2	150.4	268	52	76	68	40	73	171	12	79	6	322	78
19	Aug 22	08	02	14.5	83	62.6	149.3	78	48	66	290	48	66	183	18	94	2	6	71
20	Sep 8	02	22	29.8	32	61.3	147.6	192	50	86	6	40	86	99	3	8	5	237	84
21	Dec 3	23	35	23.7	128	63.1	150.8	170	66	84	335	24	73	79	7	346	19	183	70
22	Dec 16	01	49	40.7	94	62.5	148.2	285	54	80	87	38	78	188	7	97	10	326	80
23	Dec 18	02	35	00.3	123	63.0	151.0	174	58	80	347	32	82	82	4	351	13	102	77

TABLE 3

Locations (Lat., Long.) of the short period seismic stations in central Alaska used for this study.

Serial No.	Station Name	Station Code	Lat. (°N)	Long. (°W)	Elevation (Meter)
1.	Arctic Valley	PMS	61.2	149.5	716
2.	Black Rapids	BLR	63.5	145.8	809
3.	Clear Creek Butte	CCB	64.6	147.8	183
4.	Engineer Hill	ENG	64.7	147.0	220
5.	Fort Yukon	FYU	66.5	145.2	137
6.	Gilmore	GLM	64.9	147.4	722
7.	Gilmore Creek	GIL	64.9	147.5	350
8.	Granite Mountain	GMA	65.4	161.2	858
9.	Hepp	HPP	64.8	147.9	170
10.	Houston	PWA	61.6	149.8	137
11.	Indian Mountain	IMA	66.0	153.6	1233
12.	Kodiak	KDC	57.7	152.5	13
13.	Levy	LVY	64.2	149.2	230
14.	McKinley	MCK	63.7	148.9	610
15.	Mercer	MCR	63.9	149.0	456
16.	Nenana	NEA	64.5	149.0	365
17.	Palmer	PMR	61.6	149.1	100
18.	Paxon	PAX	62.9	145.5	1034
19.	Remote	RON	62.7	150.2	470
20.	Sheep Mountain	SCM	61.8	147.3	1020
21.	Sparrevohn	SVW	61.1	155.6	730
22.	Tanana	TNN	65.2	151.9	504
23.	Tatalina	TTA	62.9	156.0	914
24.	Tolsona	TOA	62.1	146.2	909

TABLE 4

Layered crust-upper mantle model used for this study.

Depth to the Interface (km)	P-wave Velocity (km/sec)
0.0	5.84
17.6	7.05
46.0	8.07
75.7	8.29
300.7	10.39
544.8	12.58

REFERENCES

Biswas, N. N. (1973). P-wave travel-time anomalies: Aleutian-Alaska region, Tectonophysics, 19, 361-367.

Gedney, L. and E. Berg (1969a). The Fairbanks earthquake of June 21, 1967; aftershock distribution, focal mechanisms and crustal parameters, Bull. Seism. Soc. Am., 59, 73-100.

Gedney, L. and E. Berg (1969b). Some characteristics of the tectonic stress pattern in Alaska, Geophys. J.R.A.S. 17, 293-304.

Gedney, L. (1970). Tectonic stresses in southern Alaska in relationship to regional seismicity and the new global tectonics, Bull. Seism. Soc. Am., 60, 1789-1802.

Hales, A. L. and T. Asada (1966). Crustal structure in coastal Alaska, The Earth beneath the continents, Geophys. Monogr. Ser. 10, 420-432.

Jordan, J., G. Dunphy and S. Harding (1968). The Fairbanks, Alaska earthquake of June 21, 1967, Preliminary Seismological Report, U. S. Dept. of Commerce, ESSA, U. S. Coast and Geodetic Survey.

Lahr, J. C. (1974). Detailed seismic investigation of Pacific-North American plate interaction in southern Alaska, Ph.D. Thesis, Columbia Univ.

Lee, W. H. K. and J. C. Lahr (1972). HYPO 71: a computer program for determining hypocenters, magnitude and first motion pattern of local earthquakes, U. S. Geological Survey, Open-File Report.

Le Pichon, X., J. Francheteau and J. Bonnin (1973). Plate Tectonics, Elsevier Sci. Pub. Co., New York.

Stauder, W. and G. A. Bollinger (1966). The focal mechanism of the Alaska earthquake of March 28, 1964, and of its aftershock sequence, J. Geophys. Res., 71, 5283-5296.

Stauder, W. (1968a). Mechanism of the Rat Island earthquake sequence of February 4, 1965 with relation to island arc and sea-floor spreading, J. Geophys. Res., 73, 3847-3858.

Stauder, W. (1968b). Tensional character of earthquake foci beneath the Aleutian trench with relation to sea-floor spreading, J. Geophys. Res., 73, 7693-7701.

Van Wormer, J. D., J. Davies and L. Gedney (1974). Seismicity and plate tectonics in south central Alaska, Bull. Seism. Soc. Am., 64, 1467-1475.

TABLE CAPTIONS

Table 1. Locations (Lat., Long.), origin times and details of the P-wave first-motion solutions for 18 earthquakes (focal depth < 60 km) considered in this study.

Table 2. Locations (Lat., Long.), origin times and details of the P-wave first-motion solutions for 23 earthquakes (focal depth > 60 km) considered in this study.

Table 3. Locations (Lat., Long.) of the short period seismic stations in central Alaska used for this study.

Table 4. Layered crust-upper mantle model used for this study.

FIGURE CAPTIONS

Figure 1. Locations of seismic stations and epicenters of earthquakes considered for the present study.

Figure 2. P-wave first-motion solutions for earthquakes (No. 1-9) with focal depth less than 60 km. Crosses (x) indicate uncertain data points.

Figure 3. P-wave first-motion solutions for earthquakes (No. 10-18) with focal depth less than 60 km.

Figure 4. P-wave first-motion solutions for earthquakes (No. 1-12) with focal depths greater than 60 km.

Figure 5. P-wave first-motion solutions for earthquakes (No. 13-23) with focal depth greater than 60 km.

Figure 6. Relationships of the major structural trends in Alaska and first-motion solutions of the 18 earthquakes listed in Table 1. Shaded areas indicate dilatation and non-shaded areas compression. Solid arrows indicate the orientation of the pressure axis.

Figure 7. Relationships of the major structural trends in Alaska and first-motion solutions for the 23 earthquakes listed in Table 2.

Figure 8a. Composite first-motion solution for earthquakes (No. 8, 10, 11, 14 and 18).

Figure 8b. Composite first-motion solution for earthquakes (No. 4, 9, 12, 13 and 15).

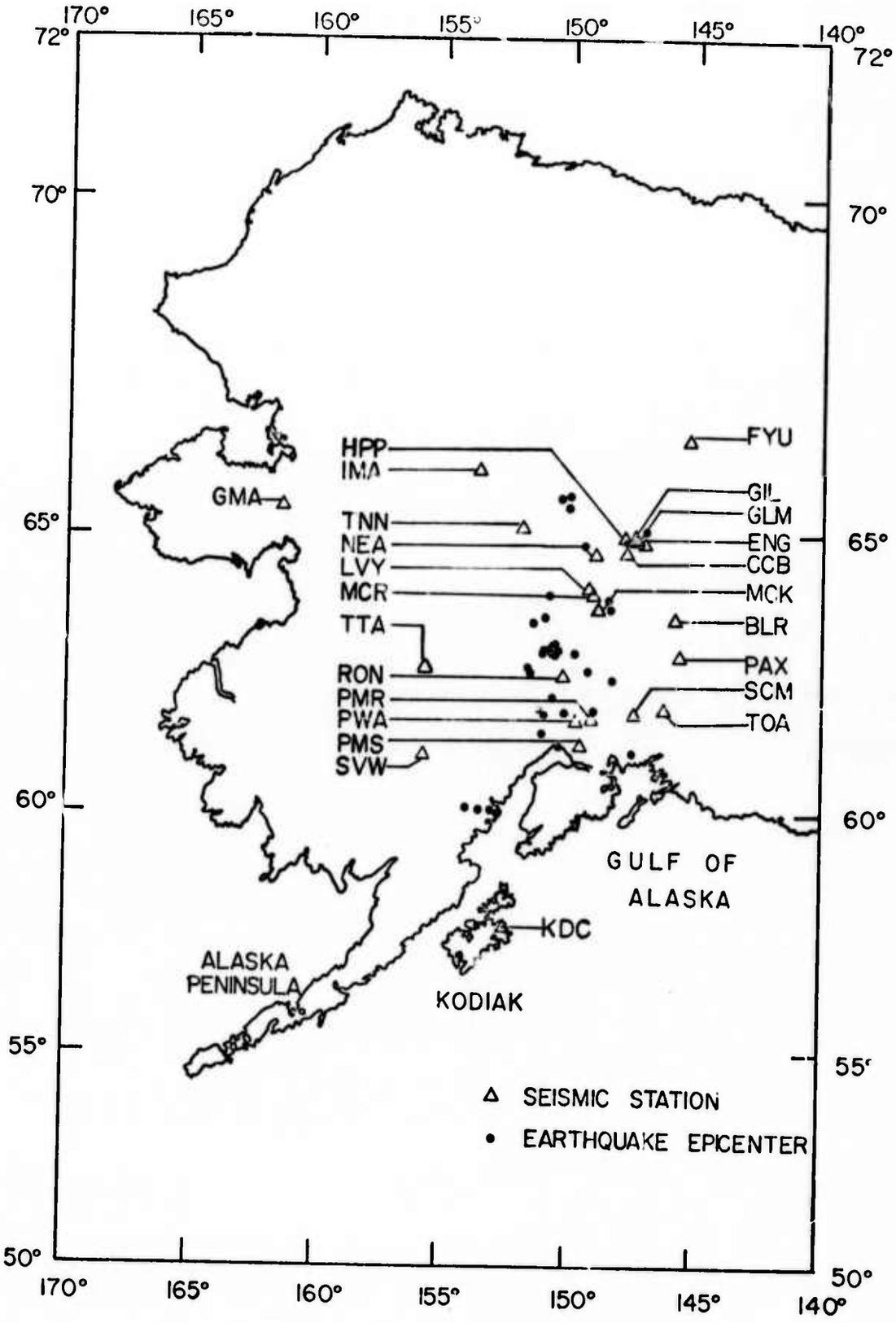

Figure 1. Locations of seismic stations and epicenters of earthquakes considered for the present study.

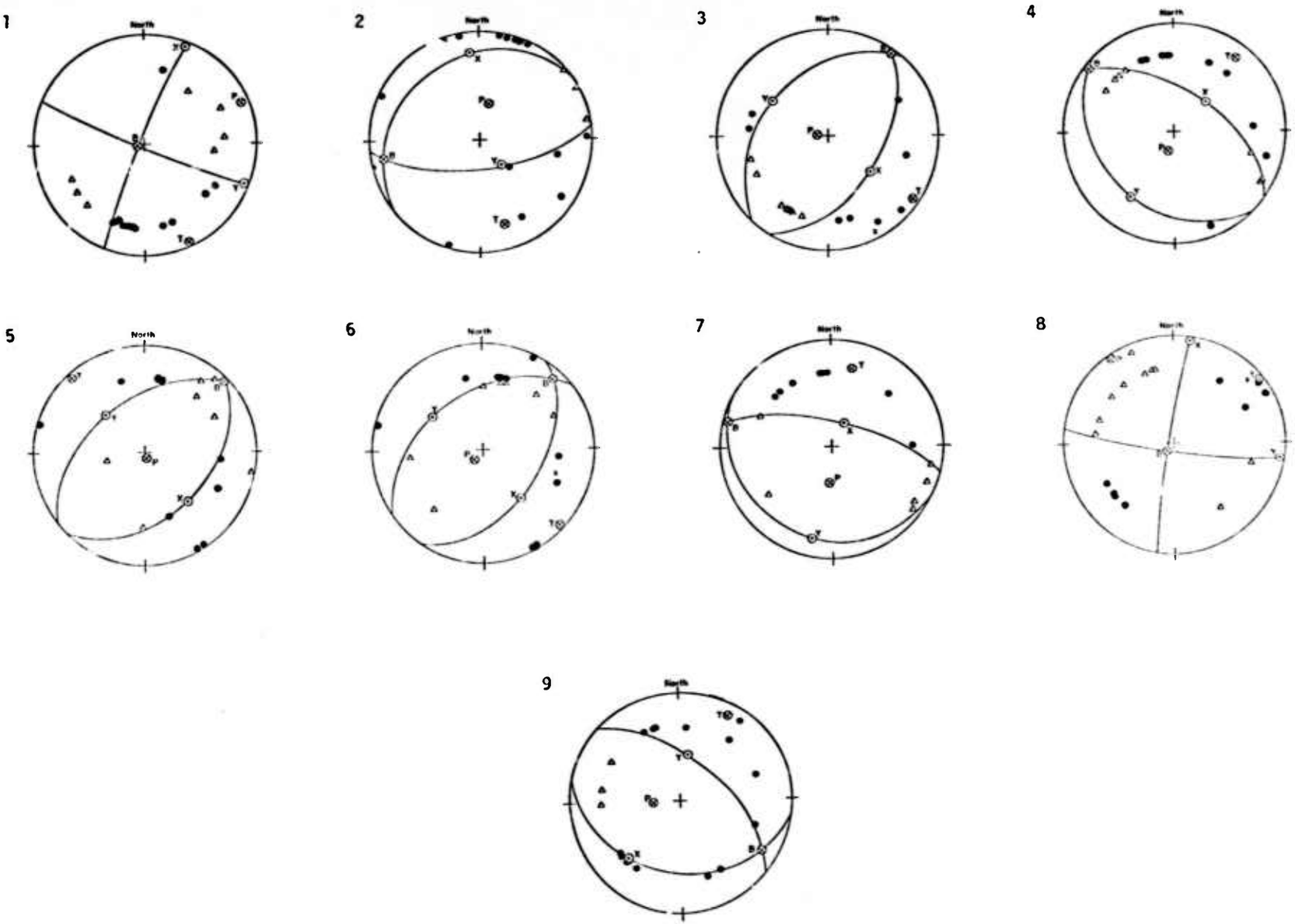

Figure 2. P-wave first-motion solutions for earthquakes (No. 1-9) with focal depth less than 60 km. Crosses (x) indicate uncertain data points.

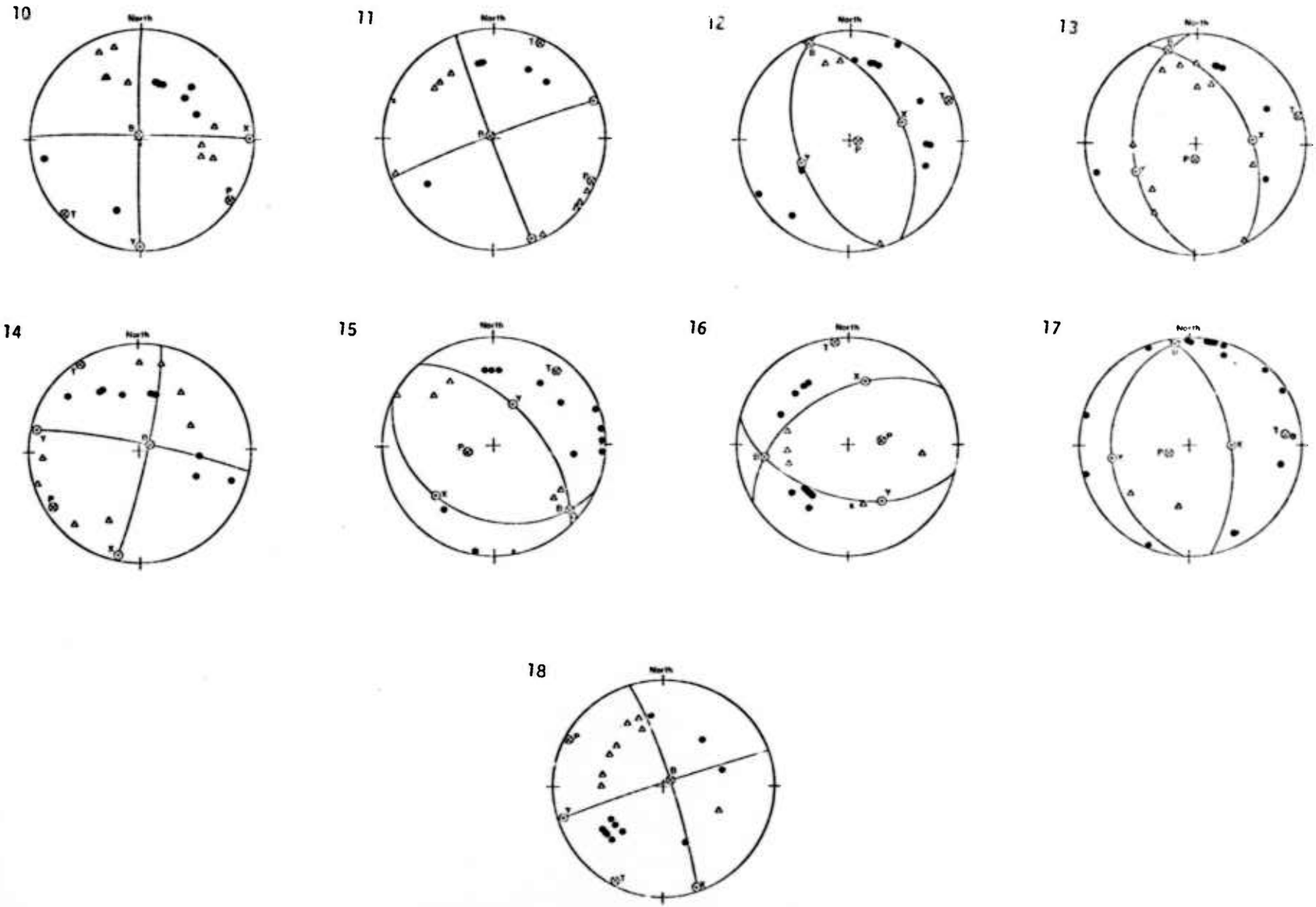

Figure 3. P-wave first-motion solutions for earthquakes (No. 10-18) with focal depth less than 60 km.

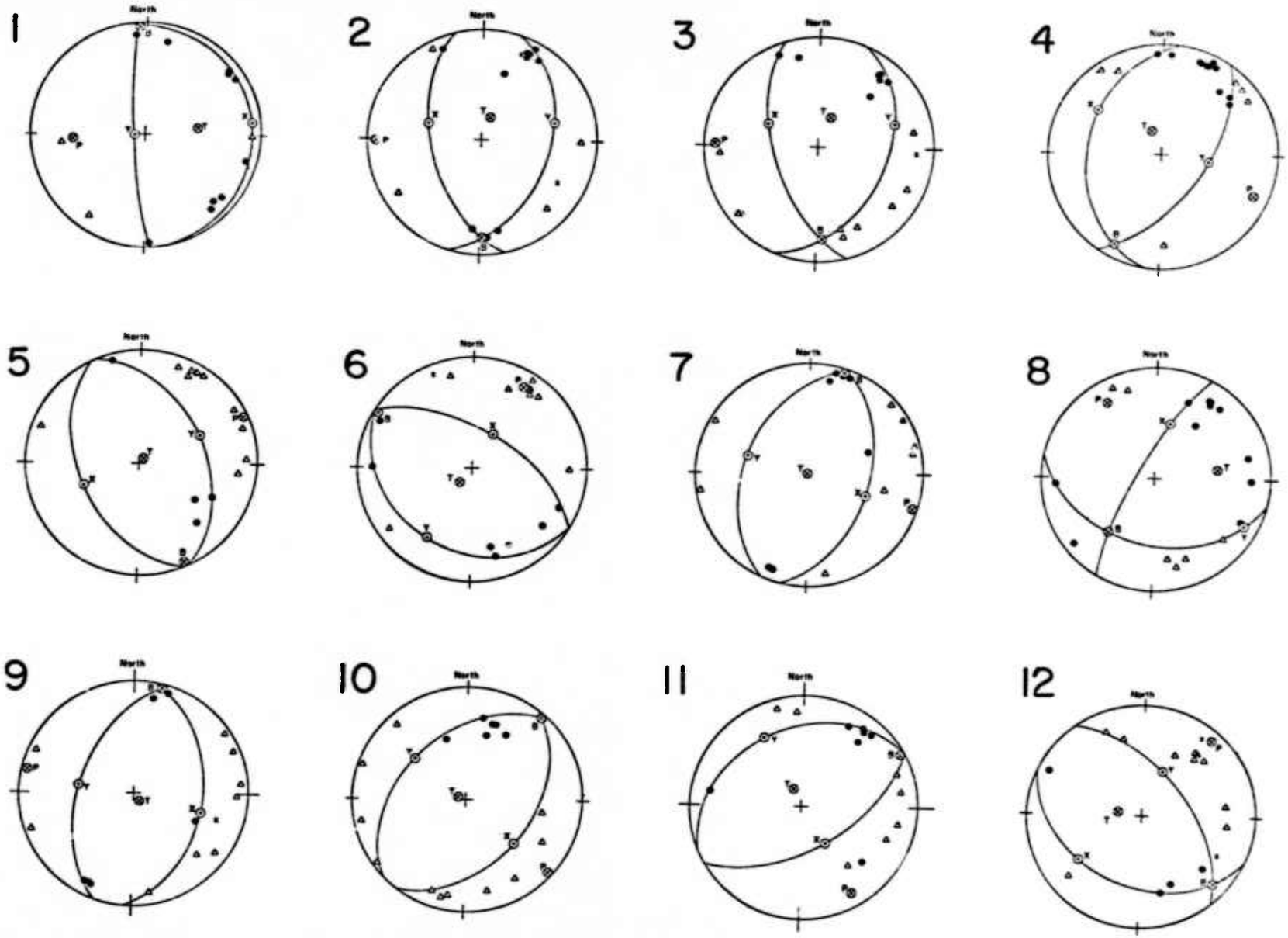

Figure 4. P-wave first-motion solutions for earthquakes (No. 1-12) with focal depths greater than 60 km.

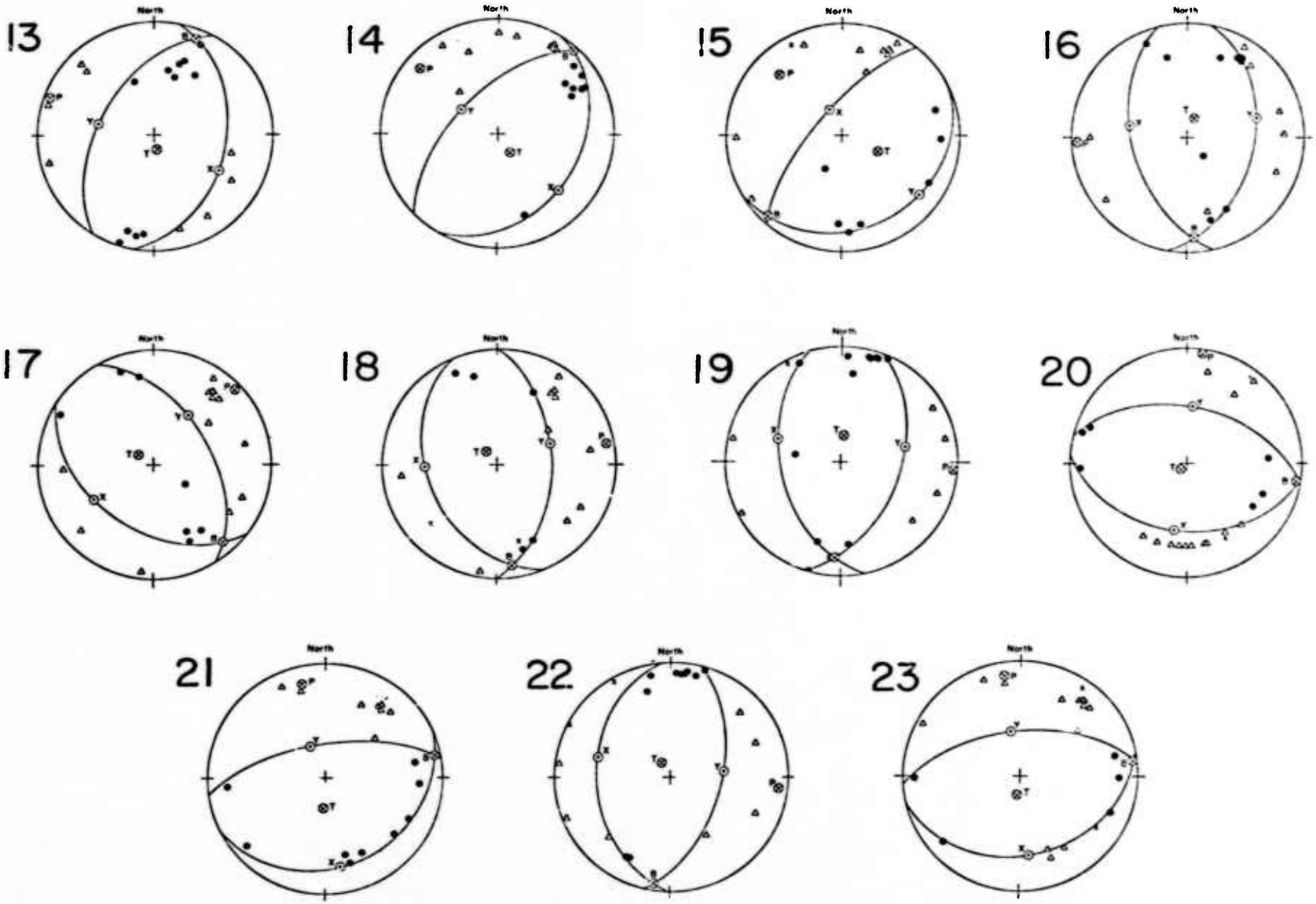

Figure 5. P-wave first-motion solutions for earthquakes (No. 13-23) with focal depth greater than 60 km.

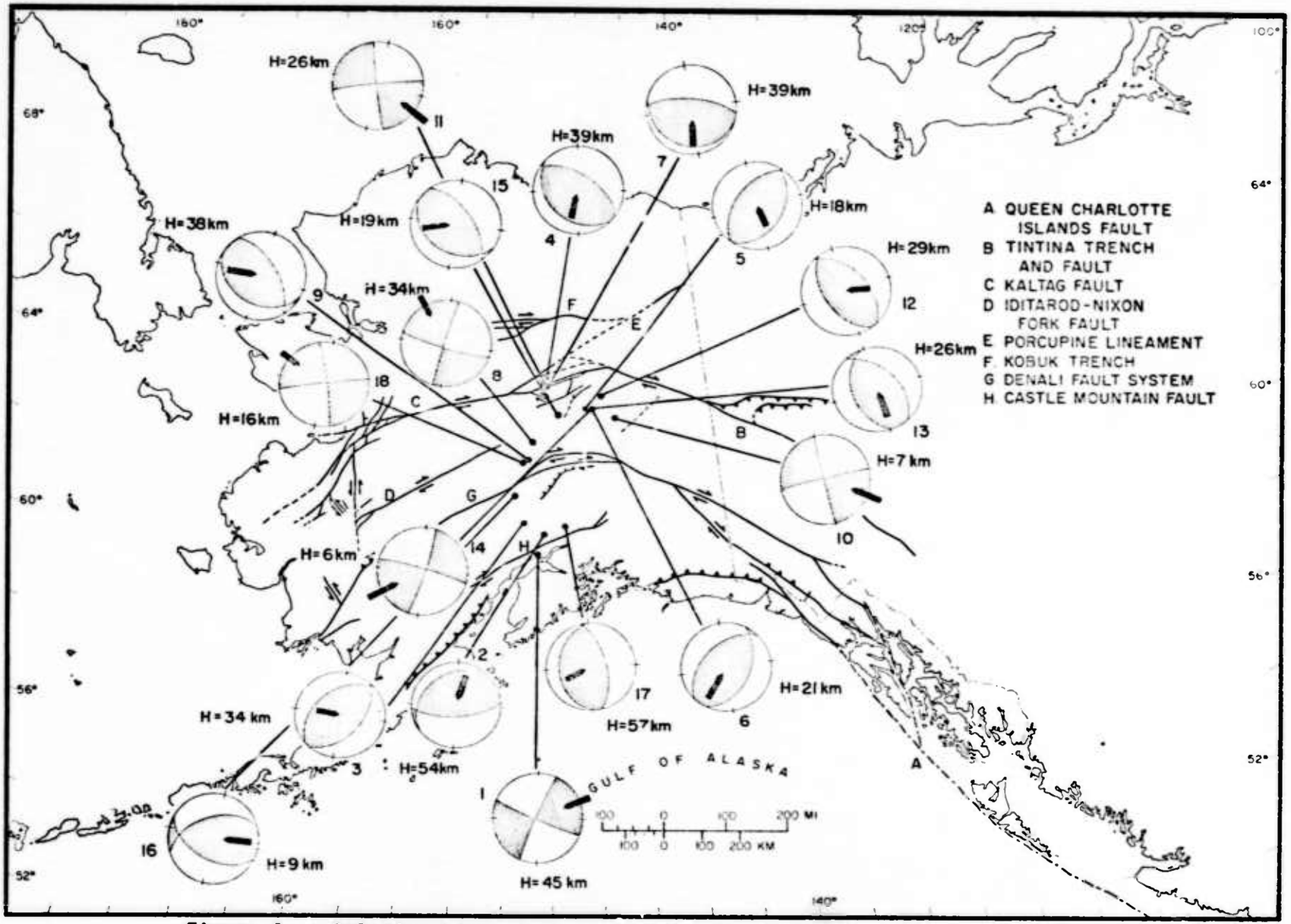

Figure 6. Relationships of the major structural trends in Alaska and first-motion solutions of the 18 earthquakes listed in Table 1. Shaded areas indicate dilatation and non-shaded areas compression. Solid arrows indicate the orientation of the pressure axis.

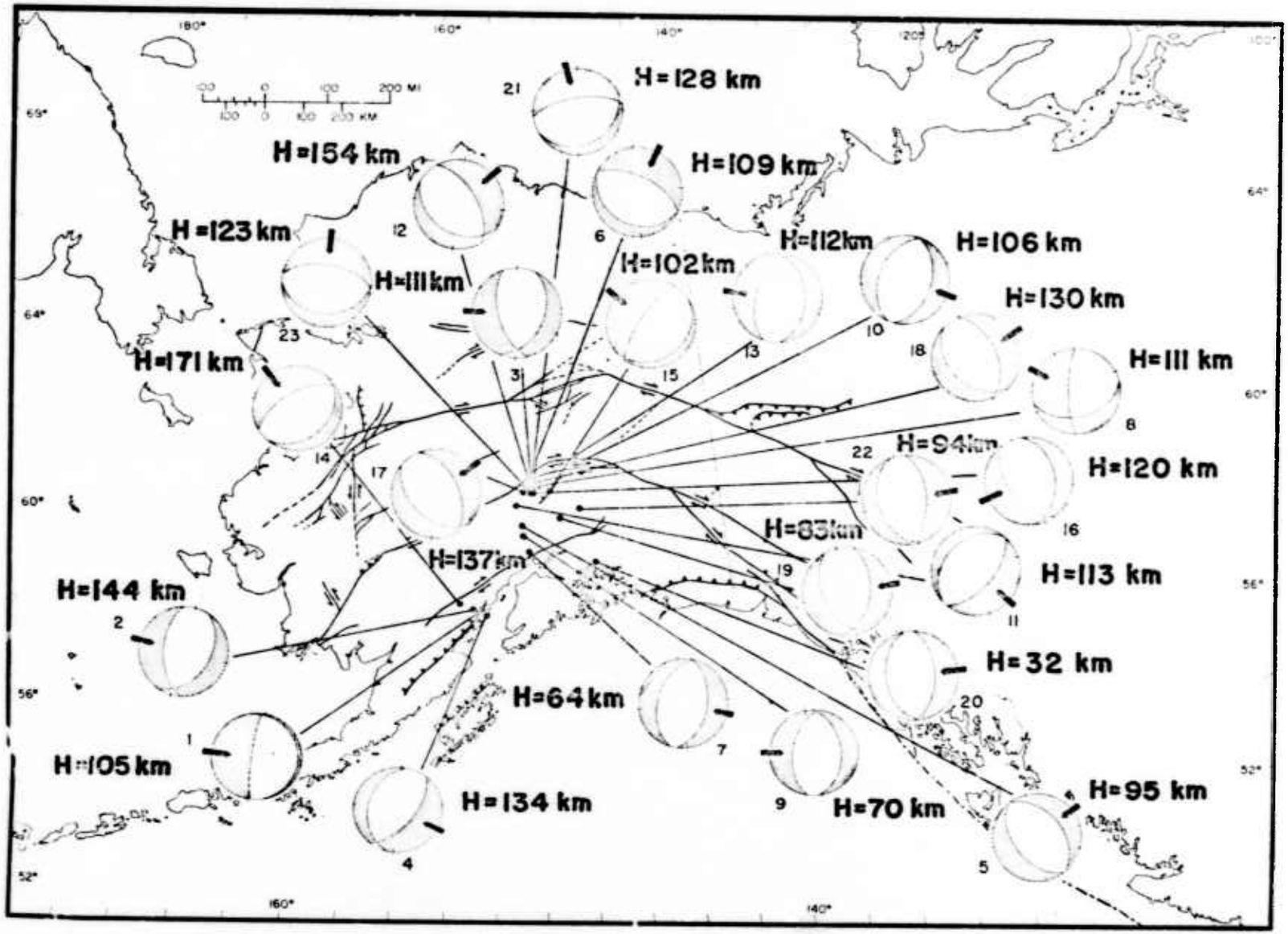

Figure 7. Relationships of the major structural trends in Alaska and first-motion solutions for the 23 earthquakes listed in Table 2.

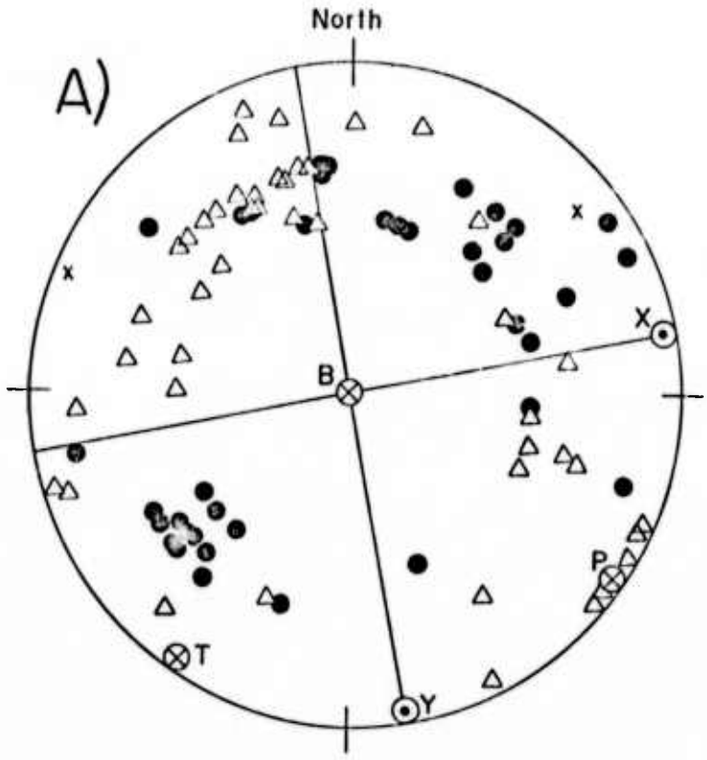

Figure 8a. Composite first-motion solution for earthquakes (No. 8, 10 11, 14 and 18).

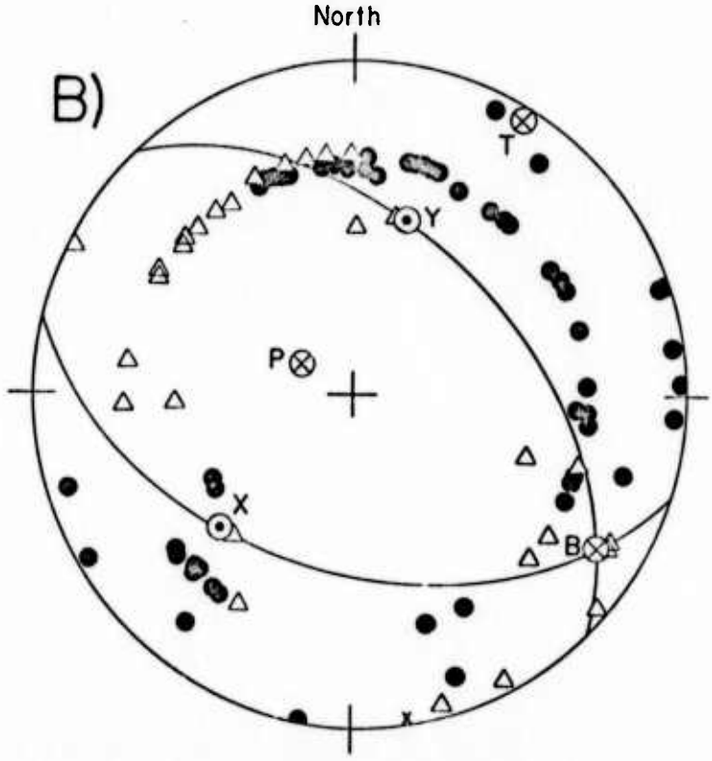

Figure 8b. Composite first-motion solution for earthquakes (No. 4, 9, 12, 13 and 15).

PAGES 69 TO BLANK

4. STUDY OF M_s-M_b RELATIONS FROM CENTRAL ALASKAN DATA

by

N. N. Biswas and B. Bhattacharya

ABSTRACT

Short and long period seismograms obtained by the standard College Observatory in central Alaska from 1968 through 1972 have been analyzed from underground explosions and earthquakes located in and around the areas of explosions for two regions: California-Nevada and the Aleutian Island chain. In the M_s-m_b relations, the results for explosions showed clear separation from those for earthquakes.

INTRODUCTION

Many authors (Liebermann and Pomeroy, 1969; Evernden et al., 1971; Ward and Toksöz, 1971) have shown from theoretical and experimental results that a significant difference in the surface wave (M_s) versus body wave (m_b) magnitude exists between earthquakes and underground explosions. Also, regional variations of M_s-m_b relationships for earthquakes have been reported from time to time. The results have been summarized by Aki (1972).

Representing an earthquake source as a displacement discontinuity across a plane, Aki (1967) showed that for an infinite, isotropic and homogeneous medium, the far-field displacement spectra can be expressed as a convolution of two terms. The first term constitutes the wave propagation properties and does not include the fault motion parameters except the direction of fault motion. The second term includes the spatial and temporal dependence of the source. Also, Aki showed that the source term decreased inversely as ω^2 beyond a corner frequency, where ω is the angular frequency. Aki identified this as the ω^2-model.

By comparing such parameters as fault length, stress drop, seismic moment, and spectral ratio for periods greater than 10 sec and M_s-m_b relations from observed data with those derived theoretically according to the ω^2-model, Aki (1972) showed close agreement between the two sets of results for earthquakes of $M_s>6$.

For $M_s<6$, results of several studies indicated disagreement with those from ω^2-model particularly for the M_s-m_b relation. Moreover, for two nearby earthquakes in the Aleutian area of similar source mechanism but of magnitude 7 and 6, the corner frequencies were found in disagreement

with the ω^2-model. These results have been reviewed by Aki (1972).

The present study was initially proposed to investigate: (1) the sources of the discrepancy between the observed and predicted results for the ω^2-model, particularly for the Aleutian earthquakes of M_s<6 and (2) regionalized M_s-m_b relations for earthquakes and underground nuclear explosions. In these investigations, we emphasized the use of the high quality local ALPA data for the surface wave part of the study. It should be noted that the above array has 90% surface wave detection capability for m_b as low as 4.5 (Harley and Heiting, 1972). However, due to non-availability and/or difficulty of getting ALPA data, the scope of this study was limited to a single standard station (College) data.

DATA

We have examined College station long-period data from 1968 through 1972 for shallow earthquakes and underground nuclear explosions located in central Asia, Nevada and central Aleutian areas. Explosions with m_b<5.7 are not recorded by the long-period components (magnification ~1500) near T~20 sec for epicentral distances Δ>2000 km. This factor further reduced the scope of the study and we have based the investigation from events located in the Nevada-California and Aleutian regions.

Initially it was planned to use central Alaskan short-period array data to calculate the mean body wave magnitude m_b from multi-station values. However, the stations were not calibrated as frequently as desired due to limitations of funding. Since large uncertainties may be introduced in m_b computations from this source, we considered short-period amplitude data only from the College station.

Evernden (1967) showed from United States short-period data that the m_b relation depends on the particular phase which arrives first at a given epicentral distance. He developed magnitude relations for a number of P-wave phases. As discussed in Section 1 of this report, the travel-time studies with central Alaskan data yielded two P-wave phases for $700 \leq \Delta \leq 2800$ km. The apparent velocities obtained for these two phases were 8.29 km/sec and 10.39 km/sec. Since appropriate relations for m_b are not available for this area, we considered the following two expressions given by Evernden (1967)

$$m_b = \log(A/T)+2\ \log\Delta-3.27 \qquad \Delta<18° \qquad (1)$$

$$m_b = \log(A/T)+4\ \log\Delta-10.35 \qquad \Delta>18° \qquad (2)$$

In the above expressions, (A/T) is the ground displacement in millimicron per sec and Δ is the epicentral distance in kilometers. Equations (1) and (2) were proposed by Evernden (1967) for P-wave phases which are associated with apparent velocities of 8.5 km/sec and 10.5 km/sec, respectively. These two P-wave phases seem to correspond to those obtained from central Alaskan data for $700 \leq \Delta \leq 2800$ km as discussed above.

For surface wave ($T \sim 20$ sec) magnitude computation, we have used the following relations (Nuttli, 1973)

$$M_s = \log(A/T)+1.66\ \log\Delta+2.6, \qquad \Delta<20° \qquad (3)$$

$$M_s = \log(A/T)+1.66\ \log\Delta+3.3, \qquad \Delta>20° \qquad (4)$$

where (A/T) is the zero-peak ground displacement in milli micron per sec and Δ is the epicentral distance in degrees.

RESULTS

Despite very careful data reduction, the body wave magnitude (m_b) computation by Equations (1) and (2) resulted in values which showed

differences in the range of $\pm$ 0.5 to $\pm$ 1 from those reported in NOAA's Monthly Bulletins (PDE). It should be noted that the reported values given in PDE are means of multi-station measurements. The above discrepancy led us to conclude, as pointed out before by Liberman and Pameroy (1969) and others, that single-station m_b determination has inherent large-scale uncertainties. Thus, we used NOAA's m_b values to investigate the M_s-m_b relations.

The computation of surface wave magnitude (M_s) by Equations (3) and (4) showed a maximum difference of $\pm$ 0.2 for those events reported in the PDE. For three central Aleutian events, the comparison is shown below.

	M_s(NOAA)	M_s(Single Station)
Cannikin	5.7	5.7
Cannikin Collapse	4.9	5.02
Milrow	5.0	4.96

Since NOAA's PDE provides M_s for few events, and as the single-station determination showed reasonable agreement with those obtained from the multi-station measurements, we used M_s values determined from College station data by Equations 1 and 2. The results of M_s-m_b plots for the Nevada-California and central Aleutian areas for earthquakes and explosions are shown in Figures 1 and 2. In these plots the M_s-m_b relation derived for the ω^2-model, and those of Gutenberg-Richter (1956) and Thirlaway-Carpenter (1966), are also shown.

In the central Aleutians the three undergound nuclear explosions show clear separation from the shallow earthquakes in the same area. The relative shift on the left of the Gutenberg-Richter line for the Cannikin collapse is in close agreement with those reported (Evernden et al., 1971) for the Benham explosion and collapse. The above authors, by comparing the amplitude

spectra for the explosion and collapse, showed that the collapses are associated with a greater proportion of long-period energy compared to the explosion. In the M_s-m_b relation, this implies that for a given M_s level, the corresponding m_b should show a relative shift toward the left and is in agreement with the results in Figure 1 and 2.

The California-Nevada earthquakes and underground nuclear explosions in Nevada show a clear separation. Moreover, the points in the M_s versus m_b relation for this area in comparison with those for the central Aleutians seem to indicate a relative shift to the left for a given M_s level. The cause of this feature is possibly related to the differential path attenuation (Ward and Toksöz, 1971); this needs further study for a complete explanation of the above phenomenon. However, it may be noted that in the summary of Aki (1972, Fig. 7), similar results as above were shown for the United States in comparison to the Aleutian-Kamchatka area.

CONCLUSIONS

In the present study we have demonstrated for both the areas considered a clear separation in the M_s versus m_b relations between underground explosions and earthquakes. We have also considered the known M_s-m_b relations (Gutenberg-Richter, Thirlaway-Carpenter and Aki's ω^2-model) in this study. So far, a best fit between these relations and the present data could not be obtained.

REFERENCES

Aki, K., (1967). Scaling law of seismic spectrum, J. Geophys. Res., 72, 1217-1231.

Aki, K., (1972). Scaling law of earthquakes source time-function, Geophys. J., 31, 3-25.

Evernden, J. F., (1967). Magnitude determination at regional and near-regional distances in the United States, Bull. of Seismol. Soc. Am., 57, 591-639.

Evenden, J. F., W. J. Best, P. W. Pomerory, T. V. McEvilly, J. M. Savino, and L. R. Sykes, (1971). Discrimination between small-magnitude earthquakes and explosions, J. Geophys. Res., 76, 8042-8055.

Gutenberg, B. and C. F. Richter, (1956). Earthquake magnitude, intensity, energy and acceleration, 2, Bull. Seismol. Soc. Am., 46, 105-145.

Harley, Tn. W. and L. N. Heiting, (1972). Preliminary evaluation of ALPA, J. Geophys., 31, 297-313.

Liebermann, R. C. and P. W. Pomeroy, (1969). Relative excitation of surface waves by earthquakes and underground explosions, J. Geophys. Res., 74, 1575-1590.

Nuttli, O. (1973). Seismic wave attenuation and magnitude relations for eastern North America, J. Geophys. Res., 78, 876-885.

Thirlaway, H. I. S. and E. W. Carpenter, (1966). Seismic signal anomalies, travel times, amplitudes, and pulse shapes, Proceedings of the VESIAC special study conference on seismic signal anomalies, travel times, amplitudes, and pulse shapes, Beaugency, France.

Ward, R. W. and M. N. Toksöz, (1971). Causes of regional variation of magnitudes, Bull. Seism. Soc. Am., 61, 649-670.

FIGURE CAPTIONS

Figure 1. M_s-m_b relations for underground explosions in Nevada and earthquakes located in Nevada-California regions.

Figure 2. M_s-m_b relations for undergound explosion in Central Aleutian and earthquakes from the neighboring regions.

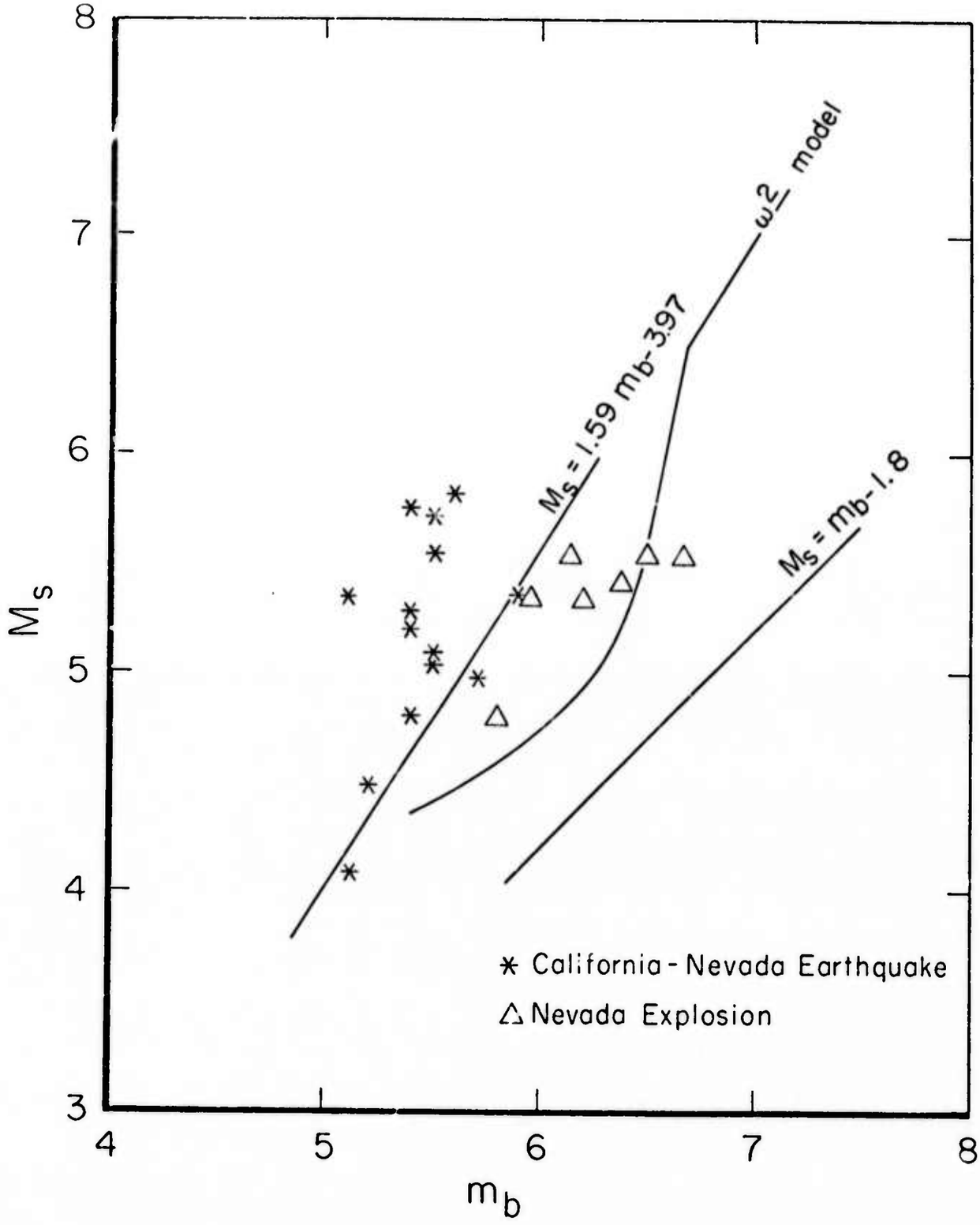

Figure 1. Ms-m_b relations for underground explosions in Nevada and earthquakes located in Nevada-California regions.

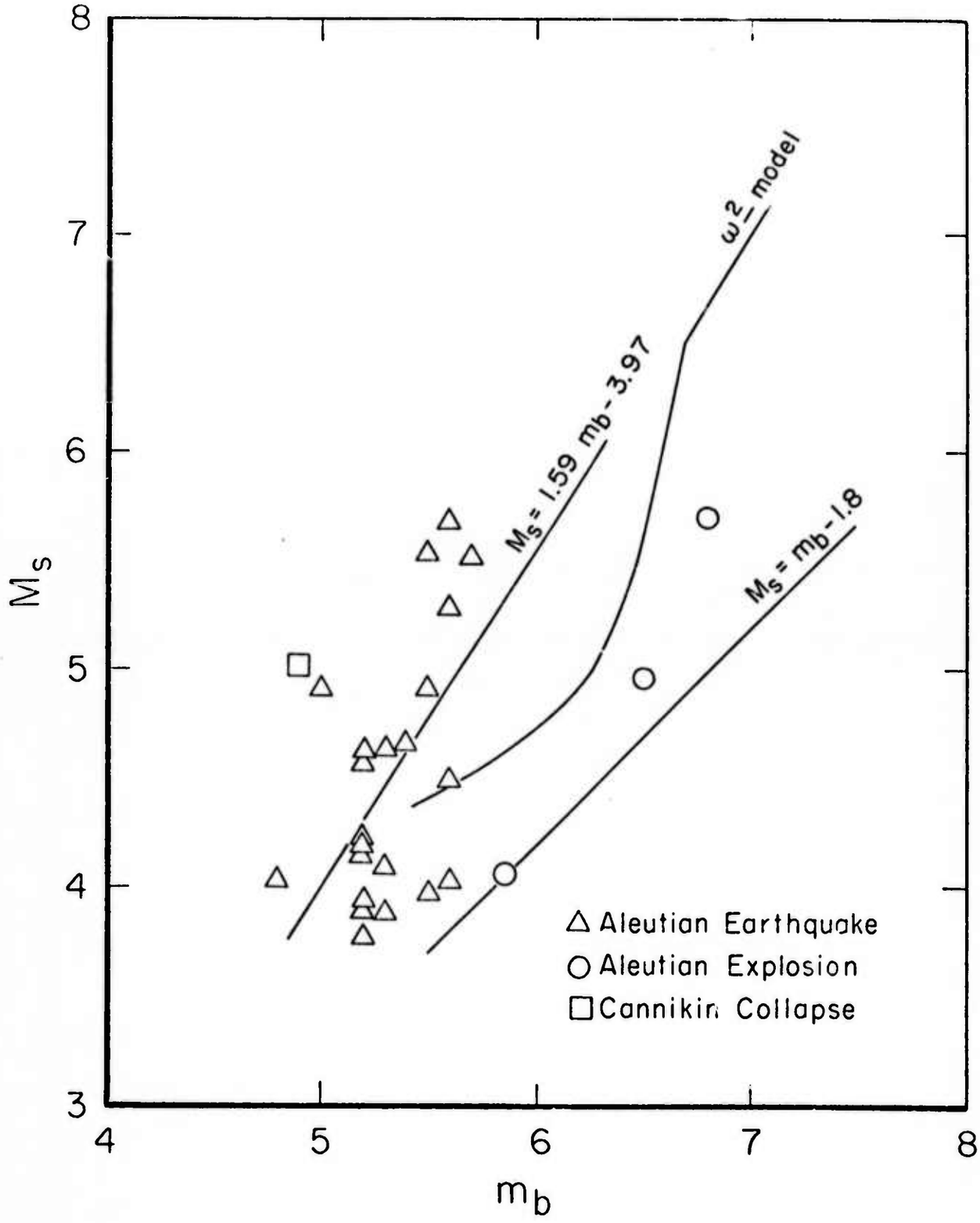

Figure 2. Ms-m_b relations for underground explosion in Central Aleutian and earthquakes from the neighboring regions.